Geologic Controls on Submarine Slope Failure along the central U.S. Atlantic Margin: Insights from the Currituck Slide Complex

Jenna C. Hill[1]*, Daniel S. Brothers[2], Bradley K. Craig[1], Uri S. ten Brink[3], Jason D. Chaytor[3], Claudia H. Flores[3]
[1]School of Coastal and Marine Systems Science, Coastal Carolina University, Conway, SC 29526
[2]Pacific Coastal and Marine Science Center, U.S. Geological Survey, Santa Cruz, CA 95060
[3]Woods Hole Coastal and Marine Science Center, U.S. Geological Survey, Woods Hole, MA 02543
****Corresponding Author: jchill@coastal.edu***

Abstract

Multiple styles of failure, ranging from densely spaced, mass transport driven canyons to the large, slab-type slope failure of the Currituck Slide, characterize adjacent sections of the central U.S. Atlantic margin that appear to be defined by variations in geologic framework. Here we use regionally extensive, deep penetration multichannel seismic (MCS) profiles to reconstruct the influence of the antecedent margin physiography on sediment accumulation along the central U.S. Atlantic continental shelf-edge, slope, and uppermost rise from the Miocene to Present. These data are combined with high-resolution sparker MCS reflection profiles and multibeam bathymetry data across the Currituck Slide complex. Pre-Neogene allostratigraphic horizons beneath the slope are generally characterized by low gradients and convex downslope profiles. This is followed by the development of thick, prograded deltaic clinoforms during the middle Miocene. Along-strike variations in morphology of a regional unconformity at the top of this middle Miocene unit appear to have set the stage for differing styles of mass transport along the margin. Areas north and south of the Currituck Slide are characterized by oblique margin morphology, defined by an angular shelf-edge and a relatively steep (>8°), concave slope profile. Upper slope sediment bypass, closely spaced submarine canyons, and small, localized landslides confined to canyon heads and sidewalls

characterize these sectors of the margin. In contrast, the Currituck region is defined by a sigmoidal geometry, with a rounded shelf-edge rollover and gentler slope gradient (<6°). Thick (>800 m), regionally continuous stratified slope deposits suggest the low gradient Currituck region was a primary depocenter for fluvial inputs during multiple sea level lowstands. These results imply that the rounded, gentle slope physiography developed during the middle Miocene allowed for a relatively high rate of subsequent sediment accumulation, thus providing a mechanism for compaction–induced overpressure that preconditioned the Currituck region for failure. Detailed examination of the regional geological framework illustrates the importance of both sediment supply and antecedent slope physiography in the development of large, potentially unstable depocenters along passive margins.

Keywords: *submarine landslides; multichannel seismic data; U.S. Atlantic margin; geomorphology, unconformity, sediment supply, stratigraphy, isopach maps, slope gradient, accommodation space*

Highlights:

- Margin morphology and sediment supply are key factors in slope instability.
- Antecedent slope physiography influences sediment accumulation patterns.
- Slope prograded margins are most likely the site of large-scale slope failures.
- The Currituck Slide was preconditioned for failure by rapid sediment accumulation.
- The stratigraphy of the Currituck Slide suggests repeated failure-prone conditions.

1. Introduction

Constraining the spatial distribution of large submarine landslides is a first step towards understanding the physical processes that lead to submarine slope failure. Along passive, siliciclastic continental margins, many of the largest submarine landslides observed on the modern seafloor occur in areas of thick sediment accumulation and limited submarine canyon development (*Hampton et al*., 1996; *Locat and Lee*, 2002; *McAdoo et al.*, 2000; *Canals et al.*, 2004; *Masson et al.*, 2006; *Krastel et al.*, 2012; *Urlaub et al.*, 2013). *Twichell* et al. (2009) identified 48 distinct landslide complexes along the U.S. Atlantic Margin (USAM) across two broad morphological categories: canyon-confined landslides found on the upper slope (<1000 m water depth) and open slope-sourced landslides that originate mostly along the low gradient seafloor of the lower slope (1500-2500 m water depth) between submarine canyons (*Booth et al.*, 1988; *Twichell et al.*, 2009). Of these two classes, open slope landslides are larger and concentrated in areas containing thick Quaternary depocenters (*Twichell et al*. 2009). Along the USAM, the accumulation and distribution of many of these Quaternary depocenters appears to be determined by a combination of sediment supply to the margin (*Poag*, 1985; *Poag and Sevon*, 1989) and antecedent, pre-Quaternary margin physiography (*Brothers et al.*, 2013a,b).

Given the tsunamigenic potential of large submarine landslides (e.g., *Driscoll et al.*, 2000; *Ward*, 2001; *Lynett and Liu*, 2002; *Geist et al.*, 2009; *Grilli et al.*, 2009; *ten Brink et al.*, 2009a; 2014; *Tappin*, 2010; *Harbitz et al*., 2013), many studies have focused on determining the causes of slope failure. Numerous preconditioning factors (e.g., high sedimentation rates, compaction, and development of pore fluid overpressure) and

triggering mechanisms (e.g., seismicity, gas hydrate dissociation, and other transient stress variations) have been linked to submarine slope failures along low-gradient passive margins (*Hampton et al.,* 1996; *Locat and Lee,* 2002; *Kayen and Lee*, 1991; *O'Leary*, 1991, 1993; *Paull et al.*, 1996, *Dugan and Flemmings*, 2000; *Canals et al.,* 2004; *Sultan et al*., 2004; *Bryn et al.*, 2005; *Kvalstad et al.*, 2005; *Urlaub et al.*, 2015). Several studies describe the prevalence of glacial cycles in the timing of large passive margin landslides, where the accumulation and subsequent destabilization of Quaternary depocenters are influenced by rapid sedimentation during glacial-interglacial transitions (*Bryn et al.*, 2005; *Kvalstad et al.*, 2005), increased seismicity due to post-glacial lithospheric rebound, and/or changes in sea level (*Stewart et al*., 2000; *Owen et al.*, 2007; *Lee*, 2009; *Brothers et al.*, 2013c), and gas hydrate dissociation (*Kayen and Lee*, 1991; *Paull et al.*, 1996; *Mosher et al.*, 2004; *Maslin et al.*, 2004; *Brothers et al.*, 2014). However, the details of these potential cause and effect relationships remain poorly understood. It is particularly notable that large open-slope landslides may be found adjacent to sections of a margin dominated by canyon incision or even intact (unfailed) sections of the slope. The central USAM displays this dichotomy very well: the large, retrogressive Currituck landslide complex (*Bunn and McGregor*, 1986; *Twichell et al.*, 2009; *ten Brink et al.*, 2014) is surrounded by broad sections of slope that are characterized by dense canyon spacing (Figs. 1, 2). We propose that the antecedent margin physiography and stratigraphic framework play important, but often overlooked roles in dictating how and where potentially unstable depocenters develop.

The aim of this study is to reconstruct the stratigraphic development of the central USAM from the Neogene to present, as this time periods appears to be when distinct differences in slope morphology arose that contributed to varying styles of slope instability. Analysis of paleo-seafloor gradients and differences in sediment accumulation patterns along the margin provide insight to the subsequent development and distribution of thick Quaternary depocenters, where many of the large landslides observed along the central USAM are found.

2. Background

2.1 Conceptual models for siliciclastic margin morphology

The first-order shape of the continental shelf-edge, slope and upper rise is an important factor in understanding deep-water depositional systems and is fundamental to constraining where sediment accumulates versus where bypass is likely to occur (*Van Wagoner et al.*, 1988; *Ross et al*., 1994; *Galloway*, 1998). Previous studies have developed morphological classifications for siliciclastic passive margins (*Pratson and Haxby*, 1996; *Adams and Schlager*, 2000, *O'Grady et al.*, 2000; *Schlager and Adams*, 2001; *Brothers et al*., 2013a) that can be separated into two end-member categories. (*1*) Oblique margins are characterized by an angular shelf-edge and a steep upper slope. Such margins are linked to relatively low energy shelf-edge environments, limited sediment supply, and often display an abrupt transition from current-driven sediment mobilization to downslope gravity-driven transport. Sediment flows bypassing the steep upper slope contribute to the development of closely spaced, slope confined submarine canyons and small landslides along canyon headwalls and sidewalls. Primary depocenters along these

margins are found near the gentler gradients of the lower slope and upper rise. (*2*) In contrast, sigmoidal margin morphology is typically linked to more energetic shelf-edge environmental conditions (e.g., stronger wave and current energy) and higher sediment supply, leading to slope progradation, the development of a smooth shelf-edge rollover and gentler downslope gradients. The low gradient slopes of sigmoidal margins are expected to contain a greater volume of accumulated Quaternary sediment than the steeper and oblique margins with dense canyon spacing (*Adams and Schlager*, 2000; *O'Grady et al.*, 2000; *Schlager and Adams*; 2001; *Brothers et al.*, 2013a). The balance between these end-member morphologies is often defined by overall slope gradient (*Ross et al.*, 1994; *Brothers et al.*, 2013a). Slope oversteepening generally contributes to erosional mass-wasting and downslope gravity flows that lead to deposition and aggradation on the lower slope. As these slope fan-aprons onlap the lower slope, this deposition in turn creates a lower-gradient platform that can support thick sediment accumulation and subsequent progradation across the upper slope provided there is sufficient sediment supply (*Ross et al.*, 1994; *Brothers et al.*, 2013a).

2.2 Depositional history

As the archetype Atlantic-style passive margin, the post-rift morphology of the USAM prior to the Neogene appears to have been characterized by a broad ramp of mixed carbonate and siliciclastic deposits (*Schlee et al.*, 1979; *Schlee and Hinz*, 1987; *Mountain and Tucholke*, 1985; *Klitgord et al.*, 1988). Increased denudation of the Appalachian Mountains and perhaps changing climatic conditions led to increased terrigenous sediment delivery to the central USAM during the middle Miocene via the Paleo-

Potomac, James, Roanoke and Susquehanna Rivers (Fig. 1; *Poag*, 1978; *Klitgord et al.*, 1988; *Poag and Sevon*, 1989; *Poag and Ward*, 1993). A massive wedge of prograded middle Miocene deltaic clinoforms underlies the shelf-edge and upper to middle slope between Norfolk Canyon and Cape Hatteras, extending the shelf-edge 30-60 km seaward of its previous position (*Poag and Sevon*, 1989; *Poag and Ward*, 1993).

This rapid progradation filled most of the accommodation space on the shelf by the early Pliocene (*Schlee et al*., 1979; *Poag*, 1984). Sediment sourced from the Paleo-James and Paleo-Roanoke Rivers mostly bypassed the shelf and forced depocenters to migrate farther offshore, building large Pliocene fan-apron complexes on the continental rise (*Schlee et al.*, 1979; *Mountain and Tucholke*, 1985; *Poag*, 1984, *Poag and Sevon*, 1989; *Poag and Ward*, 1993). Across much of the margin, these deposits were dissected during the Quaternary by widespread canyon and channel incision of the slope and upper-rise (*Poag and Sevon*, 1989; *Poag and Ward*, 1993). These features, along with onlapping base-of-slope fan-apron complexes suggest slope failures and generation of mass flows were the dominant sediment transport processes during the Quaternary (*Schlee et al.*, 1979*; Poag*, 1985; *Mountain and Tucholke*, 1985; *Poag et al.*, 1992; *Twichell et al.*, 2009; *Brothers et al.*, 2013a,b).

The Paleo-James and Paleo-Roanoke rivers supplied large quantities of sediment to the margin during Quaternary sea-level lowstands (*Stanley and Swift*, 1976; *Poag and Sevon*, 1989; *Popenoe et al., 1982; Hobbs*, 2004; *Mallinson et al.*, 2010; *Thieler et al.*, 2014). Southward progradation of the Accomack Spit on the east side of Chesapeake Bay during the Pleistocene redirected drainage southward through the Bay where the combined

drainage of the Paleo- Susquehanna and Potomac Rivers likely turned offshore, delivering additional sediment to the Norfolk Canyon region (*Hobbs*, 2004). Paleochannel incisions on the inner shelf of North Carolina suggests the Paleo- James may have continued southward to converge with the Roanoke River before flowing offshore toward the site of the Currituck Slide (*Shideler and Swift*, 1972; *Swift*, 1976; *Hobbs*, 2004; *Thieler et al.*, 2014). Extensive networks of buried paleochannels are encased in Miocene through Pleistocene units on the shelf offshore of the Albemarle Sound, indicating the Roanoke River repeatedly extended to the shelf-edge above the Currituck Slide during sea-level lowstands (*Shideler and Swift*, 1972; *Popenoe et al.*, 1982).

2.3 Major submarine landslide complexes

Many studies of large submarine landslides are site specific and localized to individual failures, which often does not require an examination of the longer-term margin evolution. At the other end of the spectrum, broad-scale morphologic classifications of continental margins (e.g., considering the entire USAM as a single entity; *O'Grady*, 2000*; Adams and Schlager*, 2000) often overlook the geological and morphological variation along a particular stretch of margin that may provide insights into the processes that preconditioned slopes for failure. *Brothers et al.* (2013a) analyzed bathymetric data spanning most of the USAM and identified six distinctive geomorphic provinces that could be linked to along-strike changes in the underlying Neogene and older geologic framework. Within these provinces, five of the largest submarine landslide complexes span a range of geologic settings, including differences in Quaternary sedimentation,

substrate architecture and neotectonic process that have generated different styles of failure (*Booth et al.*, 1993; *Twichell et al.*, 2009; *Brothers et al.*, 2013a; *ten Brink et al.*, 2014).

The geomorphic characterization of *Brothers et al.* (2013a) considered the central USAM as a single category defined by an angular shelf break and a steep, narrow upper slope dissected by densely spaced slope sourced submarine canyon networks (i.e., an oblique margin; Fig. 2). However, finer-scale variations in along-strike morphology and sedimentation history suggest the shelf-edge and slope containing the Currituck Slide Complex is geomorphologically distinct and may have resulted from a different set of geological processes. Fluvial systems delivering large volumes of sediment to the shelf-edge and upper slope have dominated the Currituck margin since the Cretaceous (*Poag and Sevon*, 1989; *Poag and Ward*, 1993; *Twichell et al*., 2009). Pronounced accumulation of slope sediment, compaction-induced sediment loading and excess pore pressure conditions (*Bunn and McGregor*, 1980; *Prior et al.*, 1986; *Locat et al.*, 2009; *Twichell et al.*, 2009) may have developed in a manner similar to the glacial margin to the north, where sediment loading or glacial recharge (*Dugan and Flemmings*, 2000; *Person et al.*, 2003), and weak layers associated with deltaic strata (*O'Leary*, 1991; 1993) are believed to have contributed to large-scale slope failures (*Twichell et al.*, 2009).

The Currituck Slide complex removed and redeposited sediment over an area greater than 6500 km^2 along the continental slope and upper rise (Figs. 1, 2). The seafloor morphology resulting from a series of nested slides of translational or slab-type failure

were initially described by *Bunn and McGregor* (1980) and *Prior et al.* (1986). Two headwall scarps with ~12° slopes were identified from the seafloor bathymetry; an upper slope headwall scarp with 250 m of relief is located seaward of the shelf break between 500-700 m water depth; a lower headwall (1100 -1400 m water depth) has ~400 m of relief across a stepped scarp (Fig. 2), where differences in lithology may have allowed more resistant units to form terraces (*Prior et al.*, 1986). Stepped seafloor scarps on either side of the main evacuation zone have been suggested to indicate an additional failure plane within the main slide and highlight the influence of bedding planes on the shape of the failure surface and surrounding scarps (*Locat et al.*, 2009). Sidewall relief associated with the lower failure(s) was estimated to be much less (100-120 m), but with steeper gradients (>25°) (*Prior et al*., 1986). *Prior et al.* (1986) also noted the presence of a possible buried scarp along the southern sidewall of the lower failure. Slump faults upslope of the slide scars have been interpreted as post-failure crown cracks (*Popenoe et al.*, 1982; *Prior et al.*, 1986). The main slide scar is floored by a seaward dipping wedge of slope strata with subsurface reflections that are laterally continuous both seaward and along slope (*Bunn and McGregor*, 1980). Subbottom data presented by *Prior et al.* (1986) show an apparent basal shear surface 4-9 m below the seafloor dips seaward ~4°, congruent with the regional stratal gradient; cores collected here suggest several meters of dry, friable clay may be associated with this surface (*Bunn and McGregor*, 1980). *Bunn and McGregor* (1980) noted that subsurface horizons can be traced laterally more than 10 km under the main slide scar and are continuous under an adjacent ridge of intact strata on the lower slope, suggesting both areas formed at the same time, under similar conditions. The intact strata are composed of well-stratified, thinly layered sequences on

the south side, with fewer unconformable horizons indicative of erosion on the north side, and small-scale slumping features in the surficial sediments (*Bunn and McGregor*, 1980). Debris fans extend seaward from the slide complex in two main zones. The primary debris field to the north covers an area ~55 km wide that extends 180 km from the estimated toe of the original slope (*Locat et al.*, 2009). A secondary debris channel is observed south of the intact slope strata and appears to truncate slope canyons to the south (Figs. 1, 2).

Cores collected from the main slide scar sampled mostly silt and clay with interbedded sands, while cores from the adjacent intact slope strata recovered organic-rich silt and clay with limited sand content (*Bunn and McGregor*, 1980). Despite limited age control, the two primary slides identified from the Currituck complex are believed to have occurred sequentially in the late Pleistocene between 50 ka – 16 ka and are thought to be related to lowstand delta development associated with the James and Roanoke Rivers (*Bunn and McGregor*, 1980; *Prior et al.*, 1986; *Locat et al.*, 2009).

3. Data and Methods

1980's vintage MCS reflection profiles obtained from the USGS National Archive of Marine Seismic Surveys (NAMSS; *https://walrus.wr.usgs.gov/NAMSS/*) provide regional framework constraints for this study. Two Western Geco data sets were used for this study, W-4-82-A (WG82) and W-6-80-A (WG80), spanning the region from the Norfolk Canyon to the southern canyon failure (Fig. 1). These data were collected using a 14-airgun array with a 36-channel streamer (100 m group spacing) for a 10-50 m vertical

resolution, and up to 5 s (twt) of penetration. Additional profiles across the shelf from the U.S. Bureau of Ocean and Energy Management (BOEM) contracted surveys (B-04-82-AT, B-11-82-AT, and B-16-76-AT) were included to identify paleochannels and fluvial valleys within the study area, but are not shown here. Western Geco collected and processed (stacked, filtered and migrated) the original 2-D data. Navigational offsets within the Western Geco and BOEM data, arising from the limited positioning capabilities at the time of acquisition, were corrected by shifting the profiles to align with correlative seafloor features in the high-resolution multibeam bathymetry data. Raw multibeam bathymetry data from numerous surveys across the study region were obtained from the NOAA National Centers for Environmental Information repository (NCEI; *http://www.ngdc.noaa.gov/mgg/bathymetry/relief.html*), edited and combined into a mosaic grid at 20 m cell spacing, following the methods of *Andrews et al.* (2012).

High-resolution sparker MCS reflection profiles were acquired aboard the *M/V Tiki XIV* in 2012. More than 1000 line-km of 72-channel (6.25 m group spacing) data were acquired along the shelf edge and slope between Norfolk Canyon and the Currituck Slide (Fig. 1). A 6 kJ sparker source provided peak frequencies between 90 and 300 Hz, yielding 5–10 m vertical resolution and ~1 km of penetration. Data were sorted into common depth point gathers using *SIOSEIS* then loaded into *Promax* for standard processing (zero phase bandpass filter, trace editing, f-k filtering, velocity analysis, static correction, normal moveout, stack and constant velocity f-k migration). Migrated sections were integrated with the existing legacy data in *IHS Kingdom Suite* for interpretation.

Additional USGS legacy MCS profiles that span the study region have been correlated to borehole logs, dredge samples and exposed seafloor outcrops on the slope (*Schlee*, 1976; *Schlee et al.*, 1979; *Poag*, 1984, 1985, 1992; *Dillon and Popenoe*, 1988; *Grow et al.*, 1988; *Poag and Ward*, 1993; *Klitgord et al.*, 1994). The interpretations allow us to identify four unconformity-bounded allostratigraphic units of *Poag and Ward* (1993) throughout the study area (Fig. 3). These allostratigraphic units are as follows: Phoenix Canyon/middle Miocene unit bounded by the middle Miocene Unconformity (MMU) at the base and the upper Miocene Unconformity (UMU) above; Mey/upper Miocene unit bounded by the UMU at the base and the Pliocene Unconformity (PU) above; Toms Canyon/Pliocene unit bounded by the PU at the base and the Quaternary Unconformity (QU) above; Hudson Canyon/Quaternary unit bounded by the QU at the base and the seafloor above. These unconformity-bounded allostratrigraphic units are not equivalent to chronostratigraphic units, (i.e. not specifically defined by upper and lower bounds of each time unit, but rather are interpreted to represent total preservation of deposits from within each time period), and thus provide first-order age control on strata beneath the shelf, slope and rise.

The allostratigraphic units defined above were gridded across the study area to generate the sediment thickness isopach maps, which were converted from two-way travel time to depth using the average layer velocities from *Klitgord and Schneider* (1994). Sediment volume and average sediment thickness (total volume divided by area) were calculated from the isopach units for Areas 1 – 4 (Fig. 1b), between 200 – 2000 m water depth. For the Quaternary sediment volume and thickness calculations, an addition of the total

volume of sediment removed by the Currituck Slide (165 km^3, *Locat et al.,* 2009) was divided proportionately between Area 1 (33 km^3) and Area 2 (132 km^3), as the slide scar covers the lower slope across both these regions (Figs. 1, 2).

Representative depth-converted sections were obtained from the NAMSS repository for the detailed horizon gradient analyses of ten representative MCS profiles spanning distinct regions across the study area. For several Western Geco profiles of which depth sections were unavailable, RMS velocity functions were obtained from metadata files, converted to interval velocities (e.g., *Dix,* 1955) and used for depth conversion. The seafloor horizon and four key allostratigraphic surfaces were extracted from each of the depth-converted MCS profiles and smoothed using a (~2km) moving average filter. These smoothed profiles were used to to calculate slope gradients along each of the seismostratigraphic horizons.

4. Seafloor Morphology

The study area is divided into four sub-regions based on margin morphology (Fig. 2), as described in the following sections.

4.1. Slope Canyons (Area 1)

Area 1 is classified as an oblique morphology due to the angular shelf-edge and a steep, narrow upper slope (Figs. 2, 3, 4). The shelf indenting Norfolk Canyon defines the northern limit of Area 1 (Figs. 1, 2). Characterized by numerous small sidewall failures along the upper reaches, and thick levee development on the lower slope, this shelf-sourced canyon has served as a significant sediment conduit for detrital material derived

from the central USAM (*Forde*, 1981). South of the Norfolk Canyon, dendritic networks of slope-sourced canyons incise the slope and uppermost rise (Fig. 2; *Goff et al.*, 2001; *Brothers et al.*, 2013a,c; *Mitchell*, 2004, 2005; *Vachtman et al.*, 2013).

4.2 Currituck Slide Complex (Area 2)

The Currituck Slide Complex dominates the morphology of Area 2. New multibeam bathymetry data reveal substantially greater detail of the seafloor in and around the slide evacuation zone (Figs. 1, 2). In addition to the previously identified upper and lower headwalls, large seafloor scarps are now clearly seen landward of the upper slope headwall, on all sides of a large section of relatively intact strata on the lower slope, and bordering the main evacuation zone across the lower slope and rise (Fig. 2). Along the northern section of the primary slide scar, the relief on the upper slope headwall decreases from 250 m to ~150 m, where the uppermost strata appear to be truncated by an additional failure farther upslope, producing a U-shaped scarp with ~100 m of relief at the shelf-edge ("shelf-edge headwall" in Figs. 1, 2). The seafloor above the upper slope headwall is highly irregular, exhibiting large undulating depressions and numerous smaller seabed pockmarks between ~250-500 m water depths. More detailed morphologic structures along each of the headwalls are now visible as well. Both the shelf-edge headwall and upper slope headwall scarps are extensively gullied (Fig. 2). Some of the sidewall scarps along the lower slope show relief up to 150-200 m; higher than previously estimated by *Prior et al.* (1986). Outcropping strata between 1500-1600 m water depth form a bench that juts >800 m seaward of the lower headwall across the extensively gullied and notched scarp. Smaller scarps up to 50 m of relief are observed

within the primary evacuation zone. Between the upper and lower headwalls, the seafloor is gently sloping (~4°), relatively smooth and undissected, with occasional scattered debris blocks.

A large (10 km wide, 18 km long, 500 m thick) section of relatively intact slope strata observed on the lower slope flanks the primary slide scar (Figs. 1, 2). This feature corresponds to the intact ridge of sediment initially described by *Bunn and McGregor* (1986), which can now be observed in much greater detail. Stepped scarps on all sides of this section ('intact slope' hereafter) show variable relief (300-600 m), with extensive gullying along the steepest scarps, and scattered debris blocks along the base (Fig. 2). The uppermost sediment package within this section appears to have been removed on the northern side, where the seafloor steps down to expose more irregular bathymetry that shows evidence of channelized downslope flows on the surface of the deposit (Figs. 1, 2).

4.3 South of Currituck (Area 3)

The margin south of the Currituck Slide Complex exhibits a distinct convex slope profile and shelf-edge that protrudes several kilometers seaward relative to the surrounding regions (Figs. 2, 3, 4). The slope in the northern portion of Area 3 is characterized by small, low order, dendritic canyon heads that coalesce just below the shelf-break into steep-walled (20-40°) and flat-floored canyons (Fig. 2). The canyon interfluves in this section are characterized by small, localized failures along canyon walls. The convex upper slope seafloor morphology is more pronounced in the southern section of Area 3 (Fig. 2), where it is characterized by large, closely spaced gullies with low-order dendritic

heads that incise the upper slope and transition downslope into small slump block failures below ~1000 m water depth (Fig. 2). The upper slope across this region is covered in circular pockmarks from the shelf break down to ~400 m water depth (Fig. 2).

4.4 Southern Canyon Failure Zone (Area 4)

The southern limit of the study area, just north of Cape Hatteras, is defined by a series of shelf indentations that have been interpreted to result from large, coalesced canyon-confined failures (*Twichell et al.*, 2009). These features contribute to the steep, concave profile of the slope throughout this region (Fig. 2, 3, 4). The heads of these canyons are extensively gullied and the scarps are short, suggesting numerous small failures rather than one large event (*Twichell et al.*, 2009). These canyons have been linked to high backscatter lobes extending more than 100 km across the seafloor observed in sidescan sonar imagery (*Twichell et al.*, 2009). Linear north-south trending troughs and seafloor offsets on the lower slope suggest potential fault control across this region (*Prior et al.*, 1986; *Locat et al.*, 2009). Although no subsurface fault structures have been identified in this immediate region, growth faults within upper Miocene section are observed on a regional seismic profile just to the south (USGS Line 17; *Klitgord et al.*, 1994).

5. Substrate Architecture

5.1. Margin-scale stratigraphic framework

The following sections describe the Neogene through Quaternary stratigraphic framework across the study region, from the Norfolk Canyon to Cape Hatteras, interpreted from allostratigraphic horizons within the regional MCS profiles. The middle

Miocene Unconformity (MMU) has a relatively gentle slope gradient (< 6°) across the upper slope along most of the study region (Figs. 3, 4). A prominent increase in gradient of the MMU across the upper rise in all four areas appears to coincide with truncation of the Lower Miocene package and subcropping of Eocene strata (Fig. 3). This change in morphology is most pronounced in Area 4, where the slope gradient increases to >10° across the lower slope/upper rise (Figs. 3, 4). The shelf-edge middle Miocene deposits are thickest (>600 m) in Areas 2 and 3 (Figs. 5, 6), where large clinoform deposits downlap onto the upper Miocene Unconformity (UMU) reflector and extend seaward to >1800 m water depth across the upper slope, with little truncation along the upper boundary (Fig. 3). The middle Miocene clinoforms in Areas 1 and 4 are more shelf-edge restricted and show truncation of the most seaward strata (Figs. 3, 5). In Area 1, this truncation is initiated directly beneath the shelf edge and extends downslope to the base of the deposit (Fig. 3). In Area 4, truncation is initiated farther offshore, preserving more of the middle Miocene upper slope strata (Fig. 3). Lower slope/upper rise aprons onlap the subcropping Eocene unit across all the areas and increase in thickness to the south (Figs. 3, 5).

Most of the upper Miocene package is thin or absent along a broad swath of the outer shelf and upper slope in Areas 1 and 4 (Fig. 5). The truncated seaward face of the middle Miocene clinoforms here generated the steepest gradients (>8°) of the upper slope along the UMU (Figs. 3, 4). The UMU in Areas 2 and 3 maintained a relatively gentle gradient across the entire slope, similar to the MMU, although the steepest (~7°) portion of the profile was shifted upslope due to onlapping and burial of the subcropping Eocene strata (Figs. 3, 4, 5). This upper Miocene package appears to be truncated mid-slope beneath

Areas 3 and 4 (Figs. 3, 5). The thickest upper Miocene deposits (~500 m) are found in Area 2, where fan-aprons onlap the lower slope/upper rise (Figs. 3, 5, 6).

The steepest gradients (8-10°) of the Pliocene Unconformity (PU) are found on the upper slope in Area 1, just beneath the modern shelf-edge inflection point, which also coincides with the inflection point of the underlying MMU (Figs. 3, 4). Pliocene accumulation is greatest on the lowermost slope and upper rise, where 300-400 m thick Pliocene fan-apron deposits onlap the steepest part of the slope (Fig. 5). Relatively gentle gradients (4-7°) along the PU underlie the slope in Areas 2 and 3. Area 2 comprises a relatively thin layer of Pliocene sediment across the upper slope that shows an abrupt increase in thickness beneath the lower headwall, where the strata onlap truncated Miocene layers (Figs. 3, 5, 7). The Pliocene sediment in Area 3 is more evenly distributed across the entire slope (Figs. 3, 5). The PU gradient steepens significantly (>10°) beneath Area 4 (Fig. 4). Pliocene deposition here is similar to Area 1, with relatively thin upper slope deposits; the sediment thickness increases downslope, but is thinner than areas to the north (Fig. 5).

The Quaternary Unconformity (QU) in Areas 1 and 4 is similarly steep (<8°) beneath the upper slope (Fig. 4). The Quaternary package in Area 1 is relatively thin (<150 m) along the upper slope (Fig. 5), where small Pleistocene deltas are perched on the shelf-edge (*Hill et al.*, 2004). Thick (>400 m) Pleistocene fan-apron sequences onlap the lower slope (Figs. 3, 5). Area 4 is mantled by a relatively thin Quaternary shelf-edge cover, giving way to mounded canyon debris on the lower slope (Figs. 3, 5). Areas 2 and 3 exhibit a

more gentle (<6°) slope profile along the QU (Figs. 3, 4). Area 2 is underlain by a seaward thickening wedge of Pleistocene material characterized by continuous reflections that are truncated by steep scarps (Figs. 3, 7, 8). Intact strata of the upper rise and lower slope can be correlated with upper slope strata, suggesting that the Quaternary sediment thickness here was ~750 m prior to failure (Figs. 5, 9, 10). The largest Quaternary sediment thickness in Area 3 is found on the outer shelf to upper slope, with fan apron deposits on the lower slope (Figs. 3, 5).

5.2 Stratal Architecture of the Currituck Submarine Slide Complex

Regional mapping of the allostratigraphic surfaces described above, combined with new higher-resolution Sparker MCS data, provides additional constraints on the stratal architecture encompassing the Currituck Slide. The seismic units of *Prior et al.* (1986) can now be correlated withpre-middle Miocene strata in Unit A; upper Miocene strata in Unit B, as the middle Miocene deposit is very thin on mid-slope here; and Plio-Pleistocene strata in Units C and D; resolving some earlier discrepancies regarding the possible age of these units. Several large packages of spatially continuous strata define the stratigraphy beneath the Currituck Slide failure surface and show little or no evidence for buried submarine canyons, in contrast with surrounding regions (Figs. 2, 7, 8, 9). Headwall and sidewall scarps truncate the strata and the basal failure surfaces below the scarps appear to correspond to exposed bedding planes (Figs. 7, 8). A seaward thickening section of Quaternary strata underlies the slide scar along the middle slope and onlaps the upper slope beneath the upper slope headwall (Figs. 7, 8). Successively younger packages of intact strata landward of the upper slope headwall appear to downlap onto bedding

planes that define local failure surfaces (Fig. 7). Deformed strata, deposited above buried scarps in the Pleistocene section, correspond to an irregular seafloor surface along the intact upper slope and outer shelf (Fig. 8). Several profiles appear to show an inflection point in the Quaternary and Pliocene unconformities, directly beneath the upper and lower headwalls respectively, where the paleo-seafloor gradient becomes much steeper downslope (Figs. 4, 8).

Truncated strata within the subsurface, suggestive of multiple buried scarps, are observed both landward of the upper slope headwall in the Quaternary section and seaward of the lower headwall, in the Pliocene section (Figs. 8, 10). Numerous vertical chimney structures and offset reflections are also found throughout the slide initiation area (Fig. 8). Highly reflective, deformed Pliocene strata are observed below the more continuously stratified, seaward-thickening Quaternary wedge that defines the floor of the slide scar along the mid slope (Fig. 8). Seaward of the lower headwall, the Pliocene strata that were not removed by the most recent failure are folded and faulted (Fig. 8b). Within the trough seaward of the lower headwall, Quaternary and Pliocene strata appear to be made up of stacks of chaotic sequences separated by local bounding surfaces (Fig. 8a).

A large (10 km wide, 18 km long, 500 m thick) section of subparallel, continuous reflections along the lower slope appears to contain relatively intact strata that did not fail during formation of the Currituck Slide Complex. The intact strata flank the southern edge of the primary slide scar in water depths of 1200–1800 m (Fig. 2). Regionally continuous strata can be traced from below this intact section, both across the main slide

scar to the north and upslope to the paleo shelf-edge (Figs. 8, 9, 10). Vertical faults pierce the seafloor at a 300 m high failure scarp along the lowermost slope, which shows the greatest relief of all the stepped scarps that surround this unit (Figs. 2, 9, 10). A ~100 m thick unit made up of chaotic reflections is exposed at seafloor on the north side of this deposit and sandwiched between parallel strata on the south side (Fig. 10). Where the chaotic unit is exposed at the seafloor, the bathymetry is relatively rough, compared with neighboring stratified sections, and shows evidence of downslope, channelized flows in the bathymetry (Fig. 2). A ~150 m thick stratified section is found atop this chaotic unit to the south, where perched strata appear to be draped across buried scarps, with little evidence of internal deformation or faulting within the overlying deposit (Figs. 9, 10). Chimney structures cut across most of the intact slope strata and breach the chaotic layer, but do not appear to penetrate the overlying perched strata (Figs. 9, 10).

6. Discussion

6.1 Role of Antecedent Geology in Margin Morphology and Slope Failure

Comparison of the margin morphology and underlying stratal architecture along the central USAM suggests that localized differences in slope morphology resulting from regional unconformities, along with variations in sediment supply related to paleodrainage patterns, can have a major impact on long term margin development, driving sections of the margin to be more landslide dominant or canyon dominant. Lower sediment supply and shelf-edge depocenters lead to oblique profiles with oversteepened slopes and intense canyonization, constrained by downslope gravity flows and erosion of shelf-edge material (*Adams and Schlager*, 2000, *Schlager and Adams*, 2001; *Brothers et*

al., 2013a), similar to the margin morphology observed in Areas 1 and 4 (Fig. 11). Conversely, high sediment supply and slope depocenters, indicative of progradation, tend to lead to broad, low-gradient, sigmoidal margin profiles characterized by open slope landslides and limited canyon development, as observed within Areas 2 and 3 (Fig. 11).

The extraction and analysis of regional allostratigraphic surfaces suggests that much of the study area exhibited similar paleo-seafloor morphology characterized by a smooth shelf break and a relatively gentle slope gradient prior to the middle Miocene (Figs. 3, 4, 11). Numerous paleochannels incised across the shelf suggest the margin was dominated by fluvial sediment delivery during sea level lowstands since at least the Mid-Miocene, when large, shelf-edge deltaic clinoforms were deposited (Figs. 3, 5, 11; *Poag*, 1984, *1985*; *Poag and Sevon*, 1989; *Greenlee et al.*, 1992; *Poag and Ward*, 1993; *Poulsen et al.*, 1998; *Monteverde et al.*, 2008). Differences in the preservation of these middle Miocene clinoform deposits created distinct variations in shelf-edge and slope morphology that appear to have set the stage for differing styles of mass failure along the margin (Figs. 3, 4, 11). Erosion of the seaward face of the middle Miocene clinoforms along Areas 1 and 4 ("truncated clinoform strata" in Fig. 3) appears to have contributed to the development of an oblique margin morphology, defined by an abrupt, angular shelf-break with relatively steep downslope gradients (>8°), that helped transfer large volumes of sediment to the lower slope and upper rise (Figs. 3, 5, 11). Peripheral deposition and limited sediment delivery from the Paleo-Potomac and Paleo-Roanoke Rivers to these areas during the middle Miocene (Figs, 5, 6; *Poag and Sevon*, 1989; *Poag and Ward*, 1993) may not have been sufficient to keep pace during periods of sea level

rise. Following the slope readjustment model of *Ross et al.* (1994), sediment accumulation restricted to the shelf edge and upper slope would have led to oversteepening of the margin during subsequent lowstands, which contributed to sediment bypass along the upper slope, the development of slope-sourced canyons and preferential aggradation on the lower slope and upper rise.

Limited accommodation space along the steep, oblique slope margin meant that much of the Plio-Pleistocene sediment initially deposited on upper parts of the margin was transported offshore via mass flows through preexisting canyons or the formation of new upper slope sourced canyons (*Brothers et al.*, 2013a). This led to the build up of large Pliocene fan-apron deposits, as sediment was funneled downslope (Figs. 5, 11; *Schlee et al.*, 1979; *Poag*, 1984; *Poag and Sevon*, 1989; *Poag and Ward,* 1993). As a result, these areas are dominated by closely spaced canyon incision, sediment bypass and canyon failures, with primary accumulation on canyon interfluves of the lower slope (Figs. 2, 5).

The main morphological difference between Areas 1 and 4 is that the coalesced, shelf-edge indenting canyons in Area 4 have steeper downslope gradients along the modern seafloor relative to Area 1 (Figs. 2, 3, 4, 11). This morphology appears to have been inherited from the shape of the MMU, which is steepest along the upper slope in Area 4 (Fig. 4, 11). The smooth seafloor and lack of debris blocks downslope of the large canyons in Area 4 (Fig. 2a) suggests these features may not necessarily be canyon-confined failures as suggested by *Twichell et al.* (2009), but rather the result of downslope flows along an already oversteepened oblique margin, similar to what is observed in Area 1. A higher sediment supply from the Paleo-Roanoke River, relative to

the Paleo-Potomac contribution, likely contributed to the thicker fan-apron deposits found in Area 4 as well (Figs. 5, 6).

In contrast, Areas 2 and 3 are characterized by a sigmoidal slope profile, with smooth shelf-edge rollovers and gentler slope gradients (<6°) (Figs. 2, 3, 4, 11). Deposition from the Paleo-Roanoke River appears to have contributed significant volumes of sediment to these areas since at least the middle Miocene (Figs. 5, 6; *Shideler and Swift*, 1972; *Popenoe et al.*, 1982). Evidence of downlap and seaward pinch out in the middle Miocene clinoform strata across these regions indicates a lack of significant erosional truncation at this time (Fig. 3). This evidence implies that high sediment supply may have allowed this portion of the margin to keep pace with sea level fluctuations and maintain a near equilibrium profile that allowed for continued slope progradation (*Ross et al.*, 1994). Aggradation of the lower slope and upper rise throughout the upper Miocene and Pliocene further reduced the paleo-seafloor gradient across these areas, allowing a broad ramp to develop that would support large scale Pleistocene progradation across the entire slope (Fig. 11).

Southward diversion of the Paleo-James River and convergence with the Paleo-Roanoke flowing eastward across the shelf may have significantly intensified Quaternary sedimentation across Area 2 (Figs. 5, 6; *Poag and Sevon*, 1989; *Hobbs*, 2004; *Mallinson et al.*, 2010; *Thieler et al.*, 2014). This increase in sedimentation is particularly evident in the thick, seaward thickening wedge of Quaternary slope sediment that underlies the main Currituck failure (Figs. 3, 5, 7, 8, 11). Reconstructions of the pre-failure

morphology imply massive sediment accumulation (~750 m thick) across the slope at this time, much of which was subsequently removed by the large retrogressive submarine landslide (Fig. 11; *Bunn and McGregor*, 1980*; Prior et al.*, 1986; *Locat et al.*, 2009). This interpretation is supported by the presence of intact slope strata that can be traced regionally both upslope and across the main slide evacuation zone (Figs. 9, 10).

Area 2 is the only location along the central USAM comprised of relatively continuous, parallel strata throughout, with no evidence of canyon formation beneath the slide surface, since at least the middle Miocene (Figs. 3, 7, 8). Prior to failure, seaward progradation of the continental slope appears to have created a low gradient, sigmoidal morphology more prone to large open-slope landslides due to enhanced sediment accumulation from slope progradation, much like that of southern New England and the Hudson Apron (*Brothers et al.*, 2013a). In contrast, the well-developed, closely spaced, dendritic canyons observed in Areas 1 and 4 are consistent with long term slope canyon evolution, most likely initiated by oversteepening of the upper slope associated with the shelf-edge clinoform truncation at the start of the middle Miocene; numerous stacked canyon cut-and-fill deposits are observed within the Miocene deposits along this section of the margin (Fig. 2c). Downlapping Quaternary strata on the upper slope of Area 3 show evidence of progradation similar to Area 2, although oversteepening in the mid-slope here appears to have led to canyonization and small-scale mass failures within the Quaternary section (Fig. 3). Low-order canyons with relatively steep-sided, straight thalwegs incise much of the Quaternary section across the northern portion of Area 3, but do not cut as deeply into this deposit as is observed in Area 1 (Fig. 2c). The convex

seafloor morphology of Area 3 is most pronounced in the southern part of this area, where the thickest upper-slope Quaternary sediment accumulations occur (Figs. 4, 5). This section of the margin is characterized by gullies and rills with limited incision across the upper slope, slump block scars on the mid slope and knickpoints indicative of headward erosion on the lower slope (Fig. 2b). This morphology is consistent with the canyon initiation model proposed by *Pratson and Coakley* (1996) and suggests the development of canyons in this region may be more recent than in Areas 1 and 4. Consequently, the pattern of progradation observed in the southern portion of Area 3 may be the best analog for pre-failure, upper slope stratigraphy within Area 2.

6.2 Preconditioning Factors for Currituck Slope Failure

The most critical factor for preconditioning the Currituck Slope for failure appears to be the low gradient margin morphology developed during the Miocene that supported a substantial accumulation of slope sediment (Figs. 5, 6, 11). Thick middle Miocene sediment accumulation on the upper slope may have contributed to an initial build up of high pore pressure due to rapid sediment loading. Subsequent slope progradation associated with relatively high sediment input from the Paleo-Roanoke River allowed thick Plio-Pleistocene accumulations of spatially continuous, parallel-bedded strata that would have enhanced this overburden. These strata would have generated conditions that allowed the lateral migration of pore fluid over long distances without escaping through submarine canyon walls, unlike surrounding areas. Increased sedimentation across Currituck from the merging of the Paleo-James and Paleo-Roanoke Rivers likely led to some of the thickest Quaternary sediment deposits along the margin (Figs. 5, 6). The

resulting development of overpressure from this rapid sedimentation would have reduced shear strength and promoted failure along bedding planes within the seaward dipping Quaternary wedge. Similar conditions have been described from numerous sites along passive margins (e.g., *Dugan and Flemings*, 2000; *Canals et al.*, 2004; *Kvalstad et al.*, 2005; *Leynaud*, 2007; *Flemings et al.*, 2008; *Masson et al.*, 2010; *Dugan and Sheahan*, 2012). While gas accumulation and venting features (e.g., pockmarks and chimney structures) are common across the slide complex (Figs. 2, 8, 9, 10), it is not clear if these features developed prior to failure or what role free gas accumulation or hydrate dissociation may have played in the failure.

At least four major surface scarps are visible in the surface morphology of the Currituck Slide complex (Fig. 2). The new multibeam bathymetry suggests that features interpreted as crown cracks and slump faults above upper slope headwall (*Popenoe et al.*, 1982; *Prior et al.*, 1986) appear to coincide with the irregular seafloor topography and large depressions observed at the shelf-break. These depressions exhibit a similar size and shape to the u-shaped failure observed along the northern portion of the upper slope headwall, and are underlain by possible buried scarps (Fig. 8), which suggests potential subsurface control on the position of these features. Possible buried scarps are also observed in the Pliocene section beneath the lower headwall where folded strata appear to represent an anticlinal hinge (Figs. 8b, 10). Differential compaction across similar features has been highlighted as a key factor in landslide triggering of low gradient mid slope sediments elsewhere, as this may also enhance the development of overpressured regions (e.g., *Georgiopoulou et al.*, 2007; 2010).

The upper section of intact strata on the lower slope adjacent to the Currituck Slide Complex shows evidence of well-stratified sediment perched atop channelized flows that appear as chaotic, possible mass transport deposits in the seismic section (Figs. 2, 9, 10) that may be associated with failure along one of the buried scarps. In addition, the Pliocene and Quaternary sections beneath the lower headwall show evidence of repeated layering of chaotic deposits that could be interpreted as additional mass transport deposits (Fig. 8). This evidence all suggests that this region has repeatedly developed failure-prone conditions, with multiple triggering events, since at least Pliocene time, when large-scale deposition was initiated across the slope.

7. Conclusions

The large size of the Currituck failure complex is remarkable along this portion of the central USAM, as oversteepening along much of the adjacent margin has led to closely spaced canyons fed by downslope flows and sediment bypass. Distinct differences in the modern slope morphology along this section of the central USAM appear to be inherited from antecedent physiography defined by the shape of the upper Miocene Unconformity. The development of two end members of margin morphology (sigmoidal vs. oblique) appears to have influenced the spatial distribution of sediment accumulation and the nature of slope failure within each end member. Oversteepening of the upper slope along more oblique sections of the margin generated intense canyonization in Areas 1 and 4. In contrast, rapid sedimentation and continued progradation of the low-gradient Currituck

margin throughout the Pliocene and Quaternary most likely led to a vast region of pore fluid overpressure within spatially continuous slope strata, preconditioning this portion of the margin for large-scale slope failure.

These morphological differences derived from variations in depositional history highlight the need to examine the subsurface architecture to better understand the evolution of continental margins through sedimentary processes. Key insights from the stratigraphic evolution of the central USAM suggest that large-scale slope failures are associated with regionally extensive depocenters along slope prograded margins that can support thick sediment accumulation along low gradient slopes. As result, these areas may be where the greatest submarine landslide hazard exists. Elsewhere, steep, oblique slopes have led to extensive canyon formation, which leads to sediment bypass and deposition on the lower slope and rise, where smaller failures occur. High rates of sediment accumulation along the slope and rise can lead to compaction–induced pore fluid overpressure and subsequent destabilization. The presence of hydrate and/or free gas within the sediment may also contribute to non-compaction generated overpressure, although the significance of this contribution remains unclear. These results highlight the importance of examining the detailed stratigraphy of the framework geology across areas with large, low-gradient Quaternary slope depocenters prior to undertaking localized geotechnical modeling or hydrate stability analyses, as the stratigraphy will provide key insights to patterns of fluid migration and zones of potential instability. Although much of the sediment from the evacuation zone of the Currituck Slide has been dispersed, investigation of the upper slope adjacent to Currituck in Area 3 may provide significant insight into the local

preconditioning factors prior to slope failure. We suggest particular emphasis should be placed on examining the stratigraphy of this region, as well as the intact slope strata within Area 2, as these areas appear to provide the best analogs and direct records of sedimentation history and margin morphology that are comparable to the Currituck Slide Complex.

A general survey of the U.S. Atlantic margin, as well as of passive margins worldwide, suggests that the majority of large submarine slope failures are located on the lower slope/upper rise and often coincide with regions of thick Quaternary sediment accumulation (*Canals et al.*, 2004*; Mosher et al., 2004; Masson et al.*, 2006, *Twichell et al.*, 2009; *Krastel et al.*, 2012), and the Currituck Slide Complex is a prime example of this relationship. These observations highlight the need to use regional framework analyses to better understand potential locations of instability along a margin. The desired outcome of this strategy is a shift toward a predictive framework in which morphological characterization (e.g., *Adams and Schlager*, 2000; *O'Grady*, 2000; *Mosher et al.*, 2004; *Amblas et al.*, 2006; *Brothers et al.*, 2013a), landslide distribution patterns (e.g., *McAdoo et al.*, 2000; *Masson et al.*, 2006; *Twichell et al.*, 2009; *ten Brink et al*., 2009b; *Krastel et al.*, 2012) and substrate architecture of the passive margins (e.g., *Brothers et al*., 2013a; *Campbell et al.*, 2015) are combined to assess the relative vulnerability of a particular region to large-scale slope failure. Detailed mapping using large volumes of newly available, regional coverage, and legacy data will aid in the identification of thick, lower slope, Quaternary depocenters where large, open-slope landslides are most likely to occur. The continental slope north of Washington Canyon, offshore of Virginia, may

provide one such example. Preliminary examination of the seafloor bathymetry and slope stratigraphy of this region suggest a prograded slope with limited canyon development on the upper slope that appears similar to the seafloor morphology in Area 3, as well as a thick, stratified and regionally continuous deposit of Pliocene and Quaternary sediment on the mid to lower slope. Further analysis of the regional geologic framework, however, would be required to make a more thorough assessment of this and other potentially unstable regions.

Figures

Figure 1: Location maps showing the study area along the central U.S. Atlantic margin: (*a)* USGS seismic multichannel seismic (MCS) profiles used to constrain the allostratigraphic units described in this study; modern river locations are shown onshore and blue arrows denote the approximate locations of offshore paleo-fluvial valleys discussed in the text: P= Potomac River, S=Susquehanna River, J=James River, R= Roanoke River; boxes B and C indicate panel locations; Additional locations discussed in the text are abbreviated as follows: AB=Albemarle Sound, AC=Accomack Spit, CB=Chesapeake Bay; (*b*) Overview of the Western Geco MCS trackline coverage spanning the 4 distinct sectors of the margin discussed here; representative MCS profiles used in detailed gradient analyses are highlighted in red; (*c*) 2012 USGS Sparker MCS profiles over the Currituck Slide are shown in blue; Western Airgun MCS profile WG82-170 referenced in figure 7 is shown in green.

Figure 2: (*a*) Perspective view of the seafloor morphology compiled from high resolution multibeam bathymetry data sets gridded at 20 m resolution showing the major features of central U.S. Atlantic margin that are discussed in the text. The study region is divided into 4 areas based on seafloor morphology. (*b*) Detailed perspective view of the seafloor morphology encompassing the Currtiuck Slide complex and adjacent portions of the margin; (*b*) BOEM Airgun MCS profile across the upper slope shows the variability in the regional stratigraphy; the profile location is indicated by a transect from B-B' in part *a*. Allostratigraphic units following *Poag and Ward* (1993) are shown here, bounded by regional unconformities: middle Miocene Unconformity (MMU); upper Miocene Unconformity (UMU); Pliocene Unconformity (PU); Quaternary Unconformity (QU).

Figure 3: Representative Western Geco Airgun MCS profiles shown in grayscale highlight along strike variations in stratigraphy and resulting morphology among the four sectors of the margin. Locations of seismic lines are shown in Figure 1. Allostratigraphic units following *Poag and Ward* (1993) are shown here, bounded by regional unconformities: middle Miocene Unconformity (MMU); upper Miocene Unconformity (UMU); Pliocene Unconformity (PU); Quaternary Unconformity (QU).

Figure 4: (*a-e*) Depth-distance and (*f-j*) gradient-depth plots of allostratigraphic surfaces across representative profiles along the margin. See Figure 1 for profile locations. Bold curves represent the mean depth profiles and gradient profiles, while the individual profiles used are shown in the legend. The colors represent profiles from the four morphological provinces: Area 1 (blue); Area 2 (red); Area 3 (green); Area 4 (yellow).

The gray bars indicate the approximate depth of the continental slope-rise transition. All profile distances are normalized to the shelf-slope break.

Figure 5: Isopach maps of sediment thickness for allostratigraphic units (*a*) middle Miocene, (*b*) upper Miocene, (*c*) Pliocene and (*d*) Quaternary, interpreted from regional Western Geco Airgun and USGS Sparker MCS profiles. The trackline coverage is shown in gray. The black arrows indicate paleo-fluvial drainage locations interpreted from paleochannels preserved in seismic profiles across the shelf, as well as data from *Poag and Sevon*, 1989; *Hobbs*, 2004; *Mallinson et al.*, 2010; *Thieler et al.*, 2014.

Figure 6: Average sediment thickness between 200 – 2000 m water depth across each of the four areas of the central U.S. Atlantic margin referenced in the text. The height of the bars represents total sediment thickness from the middle Miocene to present for each area; the sediment thickness contribution for each time period is noted in italics, color coded and labeled as follows: Q = Quaternary (brown), P = Pliocene (pink), UM = upperMiocene (yellow) and MM = middle Miocene (orange).

Figure 7: Comparison of seismostratigraphy and data resolution between subparallel profiles of (*a*) USGS Sparker MCS data have been converted to envelope to highlight major reflections and (*b*) grayscale, full polarity Western Geco Airgun MCS data. The Sparker MCS data show much higher resolution stratigraphy of the Pliocene and Quaternary sections, while the Airgun MCS data provide stratigraphic controls on deeper units. See Figure 1 for profile locations.

Figure 8: USGS Sparker MCS dip profiles across the Currituck Slide Complex; the full profiles are shown in grayscale envelope form to highlight major reflections, while the insets show the full waveform stratigraphy. See Figure 1 for profile locations.

Figure 9: USGS Sparker MCS (*a*) dip and (*b*) strike profiles across a large section of intact strata on found on the lower slope adjacent to the Currituck Slide; the full profiles are shown in grayscale envelope form to highlight major reflections, while the insets show the full waveform stratigraphy. See Figure 1 for profile locations.

Figure 10: 3-Dimensional perspective view of the morphology of the Currituck Slide Complex showing grayscale envelope cross-sections from USGS Sparker MCS profiles across the intact section of the lower slope.

Figure 11: Schematic showing the depositional patterns associated with each allostratigraphic unit and the resulting morphology along the four areas of the central U.S. Atlantic margin referenced in the text; locations are shown in Figures 1 and 2.

Acknowledgements

We thank Jonathan Perkins for a very helpful review. The U.S. Geological Survey, the U.S. Nuclear Regulatory Commission and Coastal Carolina University funded this research. Any use of trade, firm, or product names is for descriptive purposes only and does not imply endorsement by the U.S. Government.

References

Adams, E.W., Schlager, W., 2000. Basic Types of Submarine Slope Curvature. *Journal of Sedimentary Research* 70, 814–828. doi:10.1306/2DC4093A-0E47-11D7-8643000102C1865D

Amblas, D., Canals, M., Urgeles, R., Lastras, G., Liquete, C., Hughes-Clarke, J.E., Casamor, J.L., Calafat, A.M., 2006. Morphogenetic mesoscale analysis of the northeastern Iberian margin, NW Mediterranean Basin. *Marine Geology* 234, 3–20. doi:10.1016/j.margeo.2006.09.009

Andrews, B.D., Chaytor, J.D., ten Brink, U., Brothers, D.S., Gardner, J.V., 2012. Bathymetric terrain model of the Atlantic Margin for marine geological investigations. U.S. Geological Survey Open-File Report 1266.

Booth, J., O'Leary, D., Popenoe, P., Danforth, W., 1993. US Atlantic continental slope landslides: their distribution, general attributes, and implications. US Geological Survey Bulletin 2002, 14–22.

Booth, J.S., O'Leary, D.W., Popenoe, P., Robb, J.M., McGregor, B.A., 1988. Map and tabulation of quaternary mass movements along the United States-Canadian Atlantic continental slope from 32 degrees 00 minutes to 47 degrees 00 minutes N. latitude, Miscellaneous Field Studies Map No. 2027.

Brothers, D.S., ten Brink, U.S., Andrews, B.D., Chaytor, J.D., 2013a. Geomorphic characterization of the U.S. Atlantic continental margin. *Marine Geology* 338, 46–63. doi:10.1016/j.margeo.2012.12.008

Brothers, D.S., ten Brink, U.S., Andrews, B.D., Chaytor, J.D., Twichell, D.C., 2013b. Geomorphic process fingerprints in submarine canyons. *Marine Geology* 337, 53–66. doi:10.1016/j.margeo.2013.01.005

Brothers, D.S., K.L. Luttrell, J.D. Chaytor, 2013c, SEA-LEVEL–INDUCED SEISMICITY AND SUBMARINE LANDSLIDE OCCURRENCE, *GEOLOGY*, 41, 979–982.

BROTHERS, D.S., C. RUPPEL, J. KLUESNER, J.D. CHAYTOR, U.S. TEN BRINK, J.C HILL, C. FLORES, B. ANDREWS, 2014, EVIDENCE FOR SEABED FLUID EXPULSION ALONG THE UPPER SLOPE AND OUTER SHELF OF THE U.S. ATLANTIC MARGIN, *GEOPHYSICAL RESEARCH LETTERS*, DOI:10.1002/2013GL058048.

Bryn, P., Berg, K., Forsberg, C.F., Solheim, A., Kvalstad, T.J., 2005. Explaining the Storegga Slide. *Marine and Petroleum Geology* 22, 11–19. doi: 10.1016/j.marpetgeo.2004.12.003

Bunn, A.R., McGregor, B.A., 1980. Morphology of the North Carolina continental slope, western North Atlantic, shaped by deltaic sedimentation and slumping. *Marine Geology* 37, 253–266. doi: 10.1016/0025-3227(80)90105-X

Campbell, D.C., Shimeld, J., Deptuck, M.E., Mosher, D.C., 2015. Seismic stratigraphic framework and depositional history of a large Upper Cretaceous and Cenozoic depocenter off southwest Nova Scotia, Canada. *Marine and Petroleum Geology* 65, 22–42. doi:10.1016/j.marpetgeo.2015.03.016

Canals, M., Lastras, G., Urgeles, R., Casamor, J., Mienert, J., Cattaneo, A., Debatist, M., Haflidason, H., Imbo, Y., Laberg, J., 2004. Slope failure dynamics and impacts from seafloor and shallow sub-seafloor geophysical data: case studies from the COSTA project. *Marine Geology* 213, 9–72. doi:10.1016/j.margeo.2004.10.001

Dillon, W.P., Popenoe, P., 1988. The Blake Plateau Basin and Carolina Trough, in Sheridan, R.E., Grow, J.A. (Eds.), The Atlantic Margin: U.S., Geological Society of America, Boulder, CO.

Dix, C.H., 1955. Seismic velocities from surface measurements. *Geophysics* 20, 68–86.

Driscoll, N.W., Weissel, J.K., Goff, J.A., 2000. Potential for large-scale submarine slope failure and tsunami generation along the U.S. mid-Atlantic coast. *Geology* 28, 407 – 410. doi:10.1130/0091-7613(2000)28<407:PFLSSF>2.0.CO;2

Dugan, B., Flemings, P.B., 2000. Overpressure and Fluid Flow in the New Jersey Continental Slope: Implications for Slope Failure and Cold Seeps. *Science* 289, 288–291.

Dugan, B., Sheahan, T.C., 2012. Offshore sediment overpressures of passive margins: Mechanisms, measurement, and models. Reviews of Geophysics 50. doi:10.1029/2011RG000379

Forde, E.B., 1981. Evolution of Veatch, Washington, and Norfolk Submarine Canyons: Inferences from strata and morphology. Marine Geology 39, 197–214. doi:10.1016/0025-3227(81)90072-4

Flemings, P.B., Long, H., Dugan, B., Germaine, J., John, C.M., Behrmann, J.H., Sawyer, D., IODP Expedition 308 Scientists, 2008. Pore pressure penetrometers document high overpressure near the seafloor where multiple submarine landslides have occurred on the continental slope, offshore Louisiana, Gulf of Mexico. *Earth and Planetary Science Letters* 269, 309–325. doi:doi: DOI: 10.1016/j.epsl.2007.12.005

Galloway, W.E., 1998. Siliciclastic slope and base-of-slope depositional systems: component facies, stratigraphic architecture, and classification. *AAPG Bulletin* 82, 569–595.

Geist, E.L., Lynett, P.J., Chaytor, J.D., 2009. Hydrodynamic modeling of tsunamis from the Currituck landslide. *Marine Geology* 264, 41–52. doi:10.1016/j.margeo.2008.09.005

Georgiopoulou, A., Krastel, S., Masson, D.G., Wynn, R.B., 2007. Repeated Instability Of The NW African Margin Related To Buried Landslide Scarps, in: Lykousis, V., Sakellariou, D., Locat, J. (Eds.), Submarine Mass Movements and Their Consequences: 3 International Symposium. Springer Netherlands, Dordrecht, pp. 29–36.

Georgiopoulou, A., Masson, D.G., Wynn, R.B., Krastel, S., 2010. Sahara Slide: Age, initiation, and processes of a giant submarine slide: Sahara Slide from source to sink. *Geochemistry, Geophysics, Geosystems* 11, doi:10.1029/2010GC003066

Goff, J.A., 2001. Quantitative classification of canyon systems on continental slopes and a possible relationship to slope curvature. *Geophysical Research Letters* 28, 4359–4362. doi:10.1029/2001GL013300

Greenlee, S.M., Devlin, W.J., Miller, K.G., Mountain, G.S., Flemings, P.B., 1992. Integrated sequence stratigraphy of Neogene deposits, New Jersey continental shelf and slope: Comparison with the Exxon model. *Geological Society of America Bulletin* 104, 1403–1411. doi:10.1130/0016-7606(1992)104<1403:ISSOND>2.3.CO;2

Grilli, S.T., Taylor, O.-D.S., Baxter, C.D.P., Maretzki, S., 2009. A probabilistic approach for determining submarine landslide tsunami hazard along the upper east coast of the United States. *Marine Geology* 264, 74–97. doi:10.1016/j.margeo.2009.02.010

Grow, J.A., Klitgord, K.D., Schlee, J.S., Dillon, W.P., 1988. Representative seismic profiles of U.S. Atlantic continental margin., in: Sheridan, R.E., Grow, J.A. (Eds.), The Atlantic Continental Margin, The Geology of North America. Geological Society of America, Boulder, CO.

Hampton, M.A., Lee, H.J., Locat, J., 1996. Submarine landslides. *Rev. Geophys*. 34, 33–59. doi:10.1029/95RG03287

Harbitz, C., Løvholt, F., Bungum, H., 2014. Submarine landslide tsunamis: how extreme and how likely? *Nat Hazards* 72, 1341–1374. doi:10.1007/s11069-013-0681-3

Hill, J.C., Driscoll, N.W., Weissel, J.K., Goff, J.A., 2004. Large-scale elongated gas blowouts along the U.S. Atlantic margin. *J. Geophys. Res.* 109. doi:10.1029/2004JB002969

Hobbs, C.H., 2004. Geological history of Chesapeake Bay, USA. *Quaternary Science Reviews* 23, 641–661.

Kayen, R.E., Lee, H.J., 1991. Pleistocene slope instability of gas hydrate- laden sediment on the Beaufort sea margin. *Marine Geotechnology* 10, 125–141. doi:10.1080/10641199109379886

Klitgord, K.D., Hutchinson, D.R., Schouten, H., 1988. Atlantic Continental Margin: Structural and Tectonic Framework, in Sheridan, R.E., Grow, J.A. (Eds.), The Atlantic Margin: U.S., Geological Society of America, Boulder, CO.

Klitgord, K.D., Poag, C.W., Schneider, C.M., North, L., 1994. Geophysical database of the East Coast of the United States northern Atlantic margin--cross sections and gridded database (Georges Bank Basin, Long Island Platform, and Baltimore Canyon Trough). U.S., Geological Survey Open-File Report 94-637.

Klitgord, K.D., Schneider, C.M., 1994. Geophysical database of the east coast of the United States northern Atlantic margin: Velocity analyses. U.S., Geological Survey Open-File Report 94-192.

Krastel, S., Wynn, R.B., Georgiopoulou, A., Geersen, J., Henrich, R., Meyer, M., Schwenk, T., 2012. Large-Scale Mass Wasting on the Northwest African Continental Margin: Some General Implications for Mass Wasting on Passive Continental Margins, in: Yamada, Y., Kawamura, K., Ikehara, K., Ogawa, Y., Urgeles, R., Mosher, D., Chaytor, J., Strasser, M. (Eds.), Submarine Mass Movements and Their Consequences, Advances in Natural and Technological Hazards Research. Springer Netherlands, pp. 189–199.

Kvalstad, T.J., Andresen, L., Forsberg, C.F., Berg, K., Bryn, P., Wangen, M., 2005. The Storegga slide: evaluation of triggering sources and slide mechanics. *Marine and Petroleum Geology* 22, 245–256. doi:10.1016/j.marpetgeo.2004.10.019

Lee, H.J., 2009. Timing of occurrence of large submarine landslides on the Atlantic Ocean margin. Marine Geology 264, 53–64. doi: 10.1016/j.margeo.2008.09.009

Leynaud, D., Sultan, N., Mienert, J., 2007. The role of sedimentation rate and permeability in the slope stability of the formerly glaciated Norwegian continental margin: the Storegga slide model. *Landslides* 4, 297–309. doi:10.1007/s10346-007-0086-z

Locat, J., Lee, H.J., 2002. Submarine landslides: advances and challenges. *Can. Geotech. J.* 39, 193–212. doi:10.1139/t01-089

Locat, J., Lee, H., ten Brink, U.S., Twichell, D., Geist, E., Sansoucy, M., 2009. Geomorphology, stability and mobility of the Currituck slide. *Marine Geology* 264, 28–40. doi:doi: DOI: 10.1016/j.margeo.2008.12.005

Lynett, P., Liu, P.L.-F., 2002. A numerical study of submarine-landslide-generated waves and run-up. *Proceedings of the Royal Society A* 458, 2885–2910. doi:10.1098/rspa.2002.0973

Mallinson, D., Riggs, S., Thieler, E.R., Culver, S., Farrell, K., Foster, D.S., Corbett, D.R., Horton, B., Wehmiller, J.F., 2005. Late Neogene and Quaternary evolution of the northern Albemarle Embayment (mid-Atlantic continental margin, USA). *Marine Geology* 217, 97–117. doi:10.1016/j.margeo.2005.02.030

Maslin, M., Owen, M., Day, S., Long, D., 2004. Linking continental-slope failures and climate change: Testing the clathrate gun hypothesis. *Geology* 32, 53. doi:10.1130/G20114.1

Masson, D., Harbitz, C., Wynn, R., Pedersen, G., Løvholt, F., 2006. Submarine landslides: processes, triggers and hazard prediction. *Philosophical Transactions of the Royal Society A* 364, 2009 –2039.

Masson, D.G., Wynn, R.B., Talling, P.J., 2010. Large Landslides on Passive Continental Margins: Processes, Hypotheses and Outstanding Questions, in: Mosher, D., Shipp, R.C., Moscardelli, L., Chaytor, J., Baxter, C.P., Lee, H., Urgeles, R. (Eds.), *Submarine Mass Movements and Their Consequences, Advances in Natural and Technological Hazards Research*. Springer Netherlands, pp. 153–165.

McAdoo, B., Pratson, L., Orange, D., 2000. Submarine landslide geomorphology, US continental slope. *Marine Geology* 169, 103–136. doi:10.1016/S0025-3227(00)00050-5

Mitchell, N.C., 2004. Form of submarine erosion from confluences in Atlantic USA continental slope Canyons. *American Journal of Science* 304, 590–611. doi:10.2475/ajs.304.7.590

Mitchell, N.C., 2005. Interpreting long-profiles of canyons in the USA Atlantic continental slope. *Marine Geology* 214, 75–99. doi:10.1016/j.margeo.2004.09.005

Monteverde, D.H., Mountain, G.S., Miller, K.G., 2008. Early Miocene sequence development across the New Jersey margin. *Basin Research* 20, 249–267. doi:10.1111/j.1365-2117.2008.00351.x

Mountain, G.S., Tucholke, B.E., 1985. Mesozoic and Cenozoic geology of the US Atlantic continental slope and rise. Geologic evolution of the United States Atlantic margin 293–341.

Mosher, D.C., Piper, D.J.W.P., Campbell, D.C., Jenner, K.A., 2004. Near surface geology and sediment failure geohazards of the central Scotian Slope. American Association of Petroleum Geologists Bulletin, 88, 703-723.

O'Grady, D.B., Syvitski, J.P.M., Pratson, L.F., Sarg, J.F., 2000. Categorizing the morphologic variability of siliciclastic passive continental margins. *Geology* 28, 207–210. doi:10.1130/0091-7613(2000)28<207:CTMVOS>2.0.CO;2

O'Leary, D.W., 1991. Structure and morphology of submarine slab slides: Clues to origin and behavior. *Marine Geotechnology* 10, 53–69. doi:10.1080/10641199109379882

O'Leary, D., 1993. Submarine mass movement, a formative process of passive continental margins: the Munson-Nygren landslide complex and the southeast New England landslide complex. Submarine Landslides: Selected Studies in the US Exclusive Economic Zone 2002, 23–39.

Owen, M., Day, S., Maslin, M., 2007. Late Pleistocene submarine mass movements: occurrence and causes. *Quaternary Science Reviews* 26, 958–978. doi:10.1016/j.quascirev.2006.12.011

Paull, C.K., Buelow, W.J., Ussler, W., Borowski, W.S., 1996. Increased continental-margin slumping frequency during sea-level lowstands above gas hydrate–bearing sediments. *Geology* 24, 143–146. doi:10.1130/0091-7613(1996)024<0143:ICMSFD>2.3.CO;2

Poag, C.W., 1978. Stratigraphy of the Atlantic Continental Shelf and Slope of the United States. *Annu. Rev. Earth Planet. Sci.* 6, 251–280. doi:10.1146/annurev.ea.06.050178.001343

Poag, C.W., 1984. Neogene stratigraphy of the submerged U.S. Atlantic margin. *Palaeogeography, Palaeoclimatology, Palaeoecology* 47, 103–127.

Poag, W., 1985. Geologic evolution of the United States Atlantic margin. Van Nostrand Reinhold, New York, NY.

Poag, C.W., 1992. US middle Atlantic continental rise: Provenance, dispersal, and deposition of Jurassic to Quaternary sediments. Geologic Evolution of Atlantic Continental Rises. Van Nostrand Reinhold, New York 100–156.

Poag, C.W., Sevon, W.D., 1989. A record of Appalachian denudation in postrift Mesozoic and Cenozoic sedimentary deposits of the U.S. Middle Atlantic continental margin. Geomorphology 2, 119–157. doi:10.1016/0169-555X(89)90009-3

POAG, C.W., WARD, L.W., 1993. ALLOSTRATIGRAPHY OF THE U.S. MIDDLE ATLANTIC CONTINENTAL MARGIN; CHARACTERISTICS, DISTRIBUTION, AND DEPOSITIONAL HISTORY OF PRINCIPAL UNCONFORMITY-BOUNDED UPPER CRETACEOUS AND CENOZOIC SEDIMENTARY UNITS. U.S., Geological Survey PROFESSIONAL PAPER NO. 1542.

Popenoe, P., Coward, E.L., Cashman, K.V., 1982. A regional assessment of potential environmental hazards to and limitations on petroleum development of the Southeastern United States Atlantic continental shelf, slope, and rise, offshore North Carolina. U.S., Geological Survey Open-File Report 82-136.

Poulsen, C.J., Flemings, P.B., Robinson, R.A.J., Metzger, J.M., 1998. Three-dimensional stratigraphic evolution of the Miocene Baltimore Canyon region: Implications for eustatic interpretations and the systems tract model. *Geological Society of America Bulletin* 110, 1105–1122. doi:10.1130/0016-7606(1998)110<1105:TDSEOT>2.3.CO;2

Pratson, L.F., Coakley, B.J., 1996. A model for the headward erosion of submarine canyons induced by downslope-eroding sediment flows. *Geological Society of America Bulletin* 108, 225–234. doi:10.1130/0016-7606(1996)108<0225:AMFTHE>2.3.CO;2

Pratson, L.F., Haxby, W.F., 1996. What is the slope of the U.S. continental slope? *Geology* 24, 3–6. doi:10.1130/0091-7613(1996)024<0003:WITSOT>2.3.CO;2

Prior, D.B., Doyle, E.H., Neurauter, T., 1986. The Currituck Slide, mid-Atlantic continental slope — Revisited. *Marine Geology* 73, 25–45. doi:10.1016/0025-3227(86)90109-X

Ross, W.C., Halliwell, B.A., May, J.A., Watts, D.E., Syvitski, J.P.M., 1994. Slope readjustment: A new model for the development of submarine fans and aprons. *Geology* 22, 511–514. doi:10.1130/0091-7613(1994)022<0511:SRANMF>2.3.CO;2

Schlager, W., Adams, E.W., 2001. Model for the sigmoidal curvature of submarine slopes. *Geology* 29, 883–886. doi:10.1130/0091-7613(2001)029<0883:MFTSCO>2.0.CO;2

Schlee, J., Behrendt, J.C., Grow, J.A., Robb, J.M., Mattick, R., Taylor, P.T., Lawson, B.J., 1976. Regional geologic framework off northeastern United States. *AAPG Bulletin* 60, 926–951.

Schlee, J.S., 1979. Structure of the continental slope off the eastern United States, in: Doyle, L.J., Piley, O.H. (Eds.), Geology of Continental Slopes. Society of Economic Paleontologists and Mineralogists, Tulsa, OK.

Schlee, J.S., Hinz, K., 1987. Seismic stratigraphy and facies of continental slope and rise seaward of Baltimore Canyon Trough. *AAPG Bulletin* 71, 1046–1067.

Shideler, G.L., Swift, D.J., 1972. Seismic reconnaissance of post-Miocene deposits, Middle Atlantic continental shelf—Cape Henry, Virginia to Cape Hatteras, North Carolina. *Marine Geology* 12, 165–185. doi:10.1016/0025-3227(72)90038-2

Stanley, D.J., Swift, D.J., 1976. Marine sediment transport and environmental management, in: Marine Sediment Transport and Environmental Management. John Wiley & Sons.

Stewart, I.S., Sauber, J., Rose, J., 2000. Glacio-seismotectonics: ice sheets, crustal deformation and seismicity. *Quaternary Science Reviews* 19, 1367–1389. doi:10.1016/S0277-3791(00)00094-9

Sultan, N., Cochonat, P., Canals, M., Cattaneo, A., Dennielou, B., Haflidason, H., Laberg, J.S., Long, D., Mienert, J., Trincardi, F., Urgeles, R., Vorren, T.O., Wilson, C., 2004. Triggering mechanisms of slope instability processes and sediment failures on continental margins: a geotechnical approach. *Marine Geology* 213, 291–321. doi: 10.1016/j.margeo.2004.10.011

Tappin, D.R., 2010. Submarine mass failures as tsunami sources: their climate control. *Philosophical Transactions of the Royal Society A* 368, 2417–2434. doi:10.1098/rsta.2010.0079

ten Brink, U.S., Lee, H.J., Geist, E.L., Twichell, D., 2009a. Assessment of tsunami hazard to the U.S. East Coast using relationships between submarine landslides and earthquakes. *Marine Geology* 264, 65–73. doi:10.1016/j.margeo.2008.05.011

ten Brink, U.S., Barkan, R., Andrews, B.D., Chaytor, J.D., 2009b. Size distributions and failure initiation of submarine and subaerial landslides. *Earth and Planetary Science Letters* 287, 31–42. doi:10.1016/j.epsl.2009.07.031

ten Brink, U.S., Chaytor, J.D., Geist, E.L., Brothers, D.S., Andrews, B.D., 2014. Assessment of tsunami hazard to the U.S. Atlantic margin. *Marine Geology* 353, 31–54. doi:10.1016/j.margeo.2014.02.011

Thieler, E.R., Foster, D.S., Himmelstoss, E.A., Mallinson, D.J., 2014. Geologic framework of the northern North Carolina, USA inner continental shelf and its influence on coastal evolution. *Marine Geology* 348, 113–130. doi:10.1016/j.margeo.2013.11.011

Twichell, D.C., Chaytor, J.D., ten Brink, U.S., Buczkowski, B., 2009. Morphology of late Quaternary submarine landslides along the U.S. Atlantic continental margin. *Marine Geology* 264, 4–15. doi:doi: DOI: 10.1016/j.margeo.2009.01.009

URLAUB, M., TALLING, P.J., MASSON, D.G., 2013. TIMING AND FREQUENCY OF LARGE SUBMARINE LANDSLIDES: IMPLICATIONS FOR UNDERSTANDING TRIGGERS AND FUTURE GEOHAZARD. *QUATERNARY SCIENCE REVIEWS* 72, 63–82. DOI:10.1016/J.QUASCIREV.2013.04.020

Urlaub, M., Talling, P.J., Zervos, A., Masson, D., 2015. What causes large submarine landslides on low gradient (<2°) continental slopes with slow (~0.15 m/kyr)

sediment accumulation? *Journal of Geophysical Research: Solid Earth* 120, 6722–6739. doi:10.1002/2015JB012347

Vachtman, D., Mitchell, N.C., Gawthorpe, R., 2013. Morphologic signatures in submarine canyons and gullies, central USA Atlantic continental margins. *Marine and Petroleum Geology* 41, 250–263. doi:10.1016/j.marpetgeo.2012.02.005

Van Wagoner, J.C., Posamentier, H.W., Mitchum, R.M., Vail, P.R., Sarg, J.F., Loutit, T.S., Hardenbol, J., 1988. An Overview of the Fundamentals of Sequence Stratigraphy and Key Definitions, in: Sea-Level Changes—An Integrated Approach, Special Publication 42. SEPM, pp. 109–124.

Ward, S.N., 2001. Landslide tsunami. *Journal of Geophysical Research* 106, 11201. doi:10.1029/2000JB900450

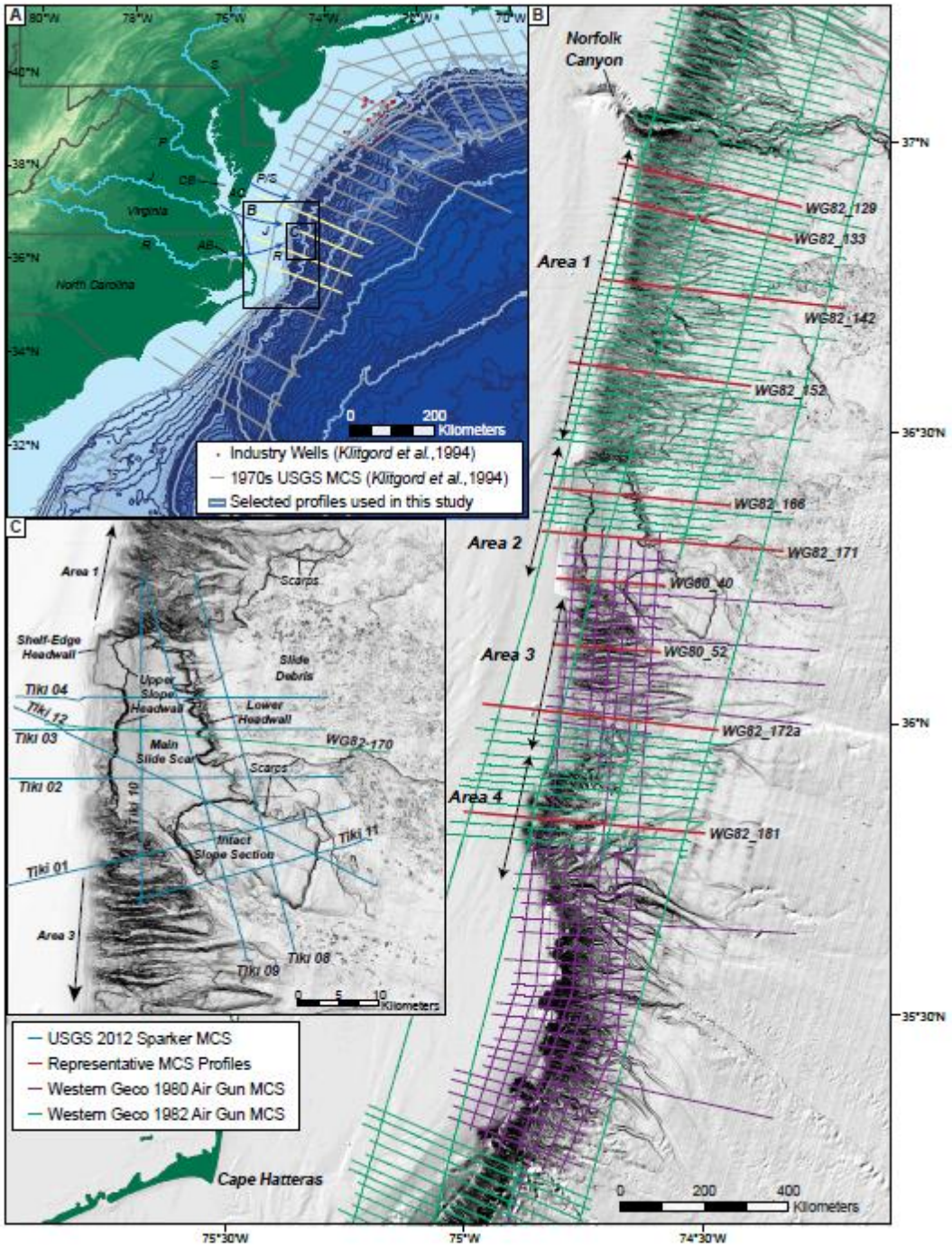
A
B
C
Norfolk Canyon
Area 1
Area 2
Area 3
Area 4
WG82_129
WG82_133
WG82_142
WG82_152
WG82_166
WG82_171
WG80_40
WG80_52
WG82_172a
WG82_181
WG82-170
Tiki 01
Tiki 02
Tiki 03
Tiki 04
Tiki 06
Tiki 08
Tiki 09
Tiki 10
Tiki 11
Tiki 12
Shelf-Edge Headwall
Upper Slope Headwall
Lower Headwall
Main Slide Scar
Slide Debris
Intact Slope Section
Scarps
Cape Hatteras
Virginia
North Carolina
Industry Wells (Klitgord et al.,1994)
1970s USGS MCS (Klitgord et al.,1994)
Selected profiles used in this study
USGS 2012 Sparker MCS
Representative MCS Profiles
Western Geco 1980 Air Gun MCS
Western Geco 1982 Air Gun MCS
Kilometers
80°W
78°W
76°W
74°W
72°W
70°W
40°N
38°N
36°N
34°N
32°N
37°N
36°30'N
36°N
35°30'N
75°30'W
75°W
74°30'W

Figure 1

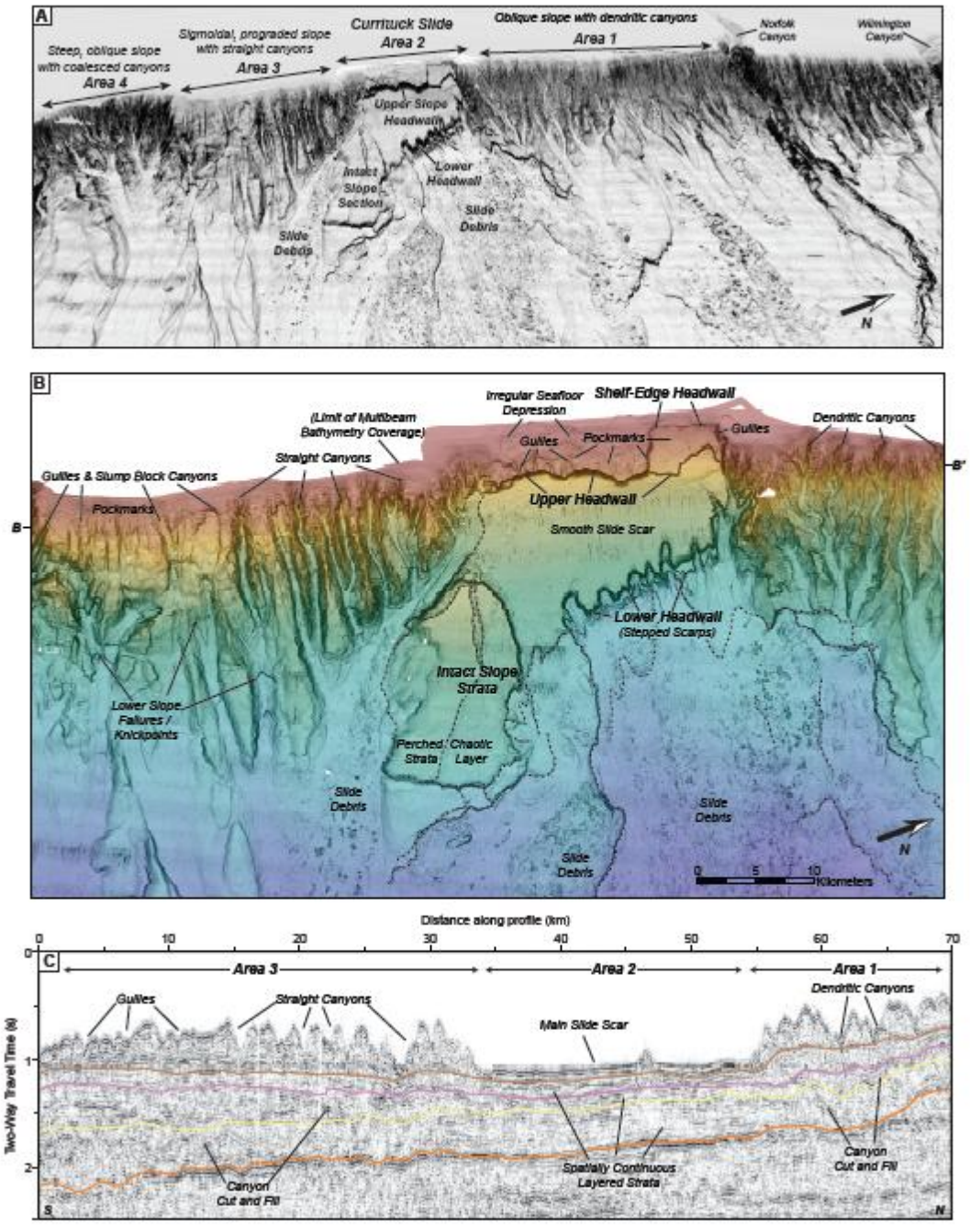
A
Steep, oblique slope with coalesced canyons
Area 4
Sigmoidal, prograded slope with straight canyons
Area 3
Currituck Slide
Area 2
Oblique slope with dendritic canyons
Area 1
Norfolk Canyon
Wilmington Canyon
Upper Slope Headwall
Intact Slope Section
Lower Headwall
Slide Debris
Slide Debris
N
B
(Limit of Multibeam Bathymetry Coverage)
Irregular Seafloor Depression
Shelf-Edge Headwall
Gullies
Pockmarks
Gullies
Dendritic Canyons
B'
Straight Canyons
Gullies & Slump Block Canyons
Pockmarks
B
Upper Headwall
Smooth Slide Scar
Lower Headwall
(Stepped Scarps)
Intact Slope Strata
Lower Slope Failures / Knickpoints
Perched Chaotic Strata
Layer
Slide Debris
Slide Debris
Slide Debris
N
0
5
10
Kilometers
Distance along profile (km)
0
10
20
30
40
50
60
70
C
Area 3
Area 2
Area 1
Gullies
Straight Canyons
Main Slide Scar
Dendritic Canyons
Two-Way Travel Time (s)
1
2
Canyon Cut and Fill
Spatially Continuous Layered Strata
Canyon Cut and Fill
S
N

Figure 2

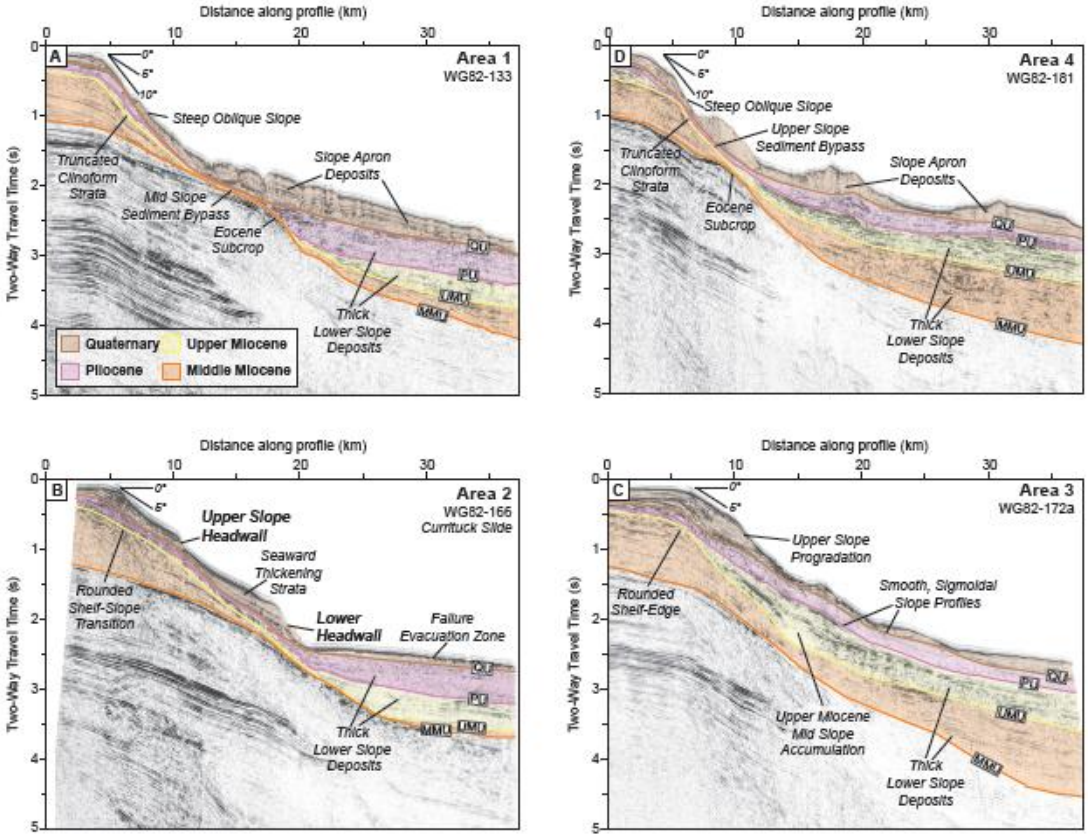
Distance along profile (km)
Two-Way Travel Time (s)
A
Area 1
WG82-133
Steep Oblique Slope
Truncated Clinoform Strata
Mid Slope Sediment Bypass
Eocene Subcrop
Slope Apron Deposits
Thick Lower Slope Deposits
Quaternary
Upper Miocene
Pliocene
Middle Miocene
D
Area 4
WG82-181
Upper Slope Sediment Bypass
B
Area 2
WG82-166
Currituck Slide
Upper Slope Headwall
Seaward Thickening Strata
Rounded Shelf-Slope Transition
Lower Headwall
Failure Evacuation Zone
C
Area 3
WG82-172a
Upper Slope Progradation
Rounded Shelf-Edge
Smooth, Sigmoidal Slope Profiles
Upper Miocene Mid Slope Accumulation

Figure 3

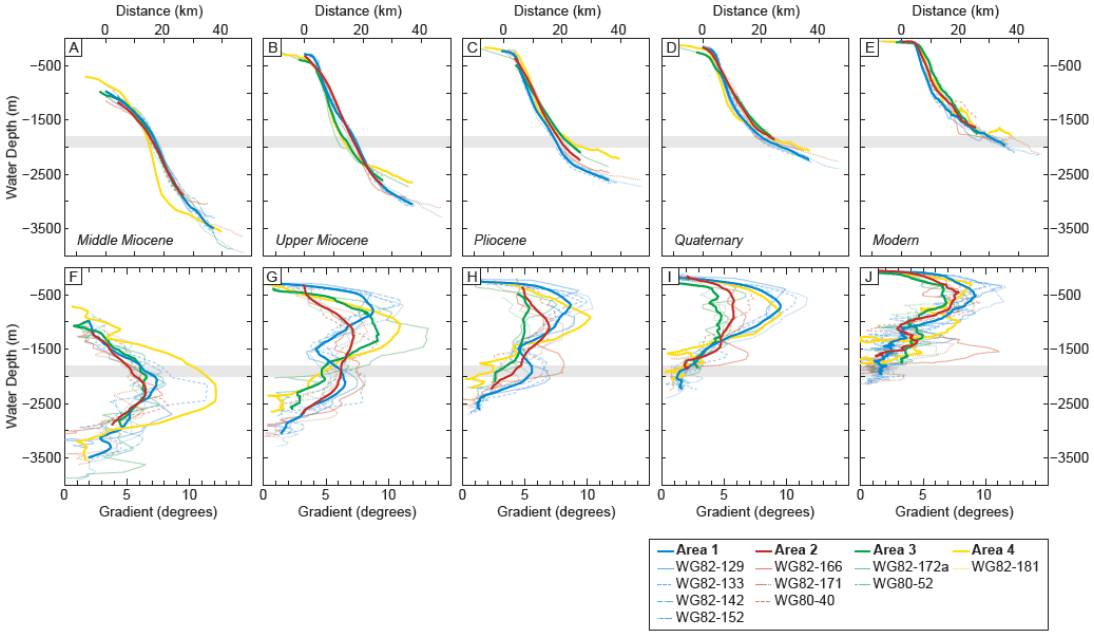
Distance (km)
0
20
40
A
B
C
D
E
Middle Miocene
Upper Miocene
Pliocene
Quaternary
Modern
Water Depth (m)
−500
−1500
−2500
−3500
F
G
H
I
J
Gradient (degrees)
0
5
10
Area 1
WG82-129
WG82-133
WG82-142
WG82-152
Area 2
WG82-166
WG82-171
WG80-40
Area 3
WG82-172a
WG80-52
Area 4
WG82-181

Figure 4

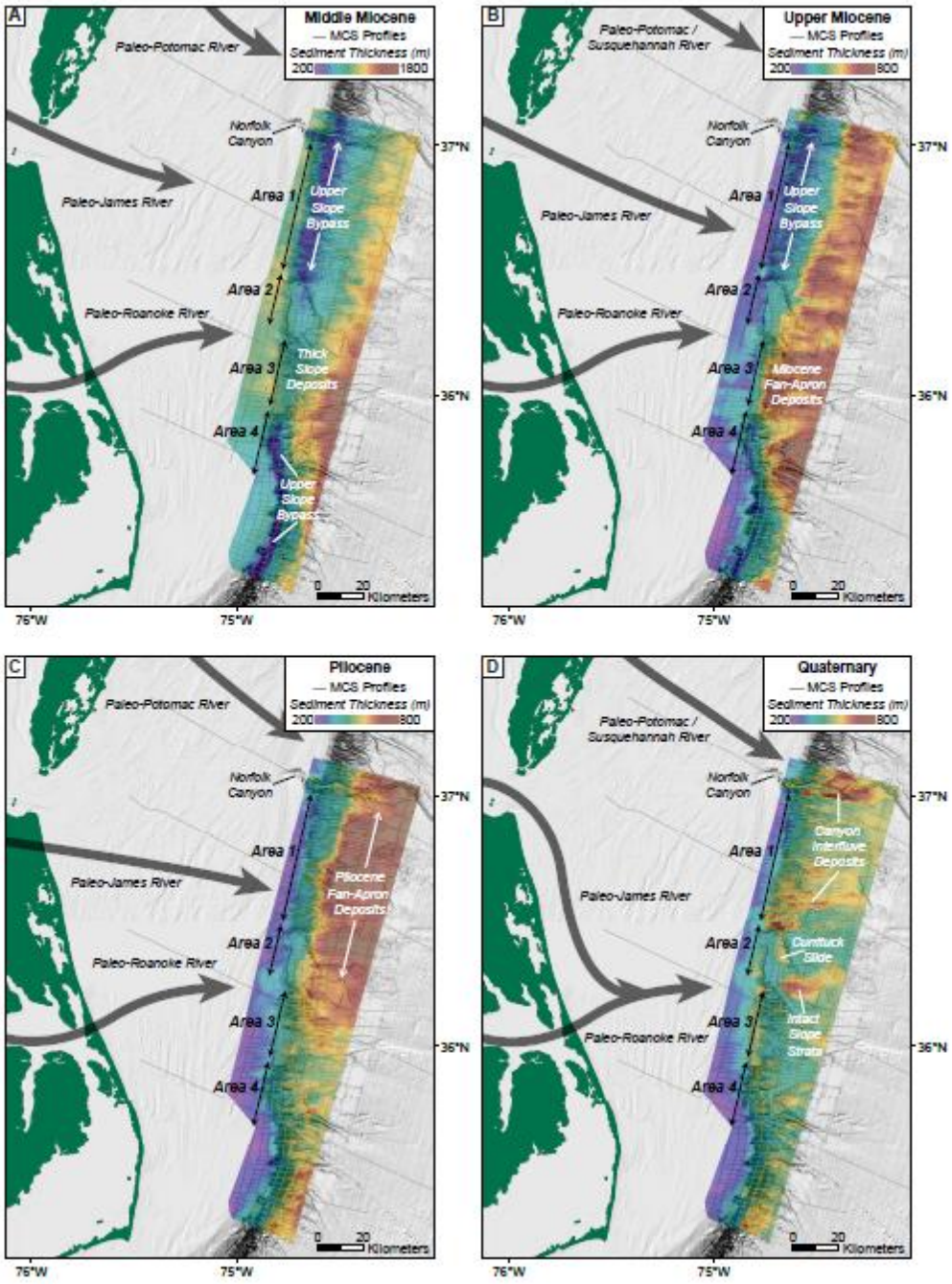
A
Middle Miocene
MCS Profiles
Sediment Thickness (m)
200
1800
Paleo-Potomac River
Norfolk Canyon
Paleo-James River
Area 1
Upper Slope Bypass
Area 2
Paleo-Roanoke River
Area 3
Thick Slope Deposits
Area 4
Upper Slope Bypass
37°N
36°N
0 20 Kilometers
76°W
75°W
B
Upper Miocene
MCS Profiles
Sediment Thickness (m)
200
800
Paleo-Potomac / Susquehannah River
Norfolk Canyon
Paleo-James River
Area 1
Upper Slope Bypass
Area 2
Paleo-Roanoke River
Area 3
Miocene Fan-Apron Deposits
Area 4
37°N
36°N
0 20 Kilometers
76°W
75°W
C
Pliocene
MCS Profiles
Sediment Thickness (m)
200
800
Paleo-Potomac River
Norfolk Canyon
Area 1
Paleo-James River
Pliocene Fan-Apron Deposits
Area 2
Paleo-Roanoke River
Area 3
Area 4
37°N
36°N
0 20 Kilometers
76°W
75°W
D
Quaternary
MCS Profiles
Sediment Thickness (m)
200
800
Paleo-Potomac / Susquehannah River
Norfolk Canyon
Area 1
Canyon Interfluve Deposits
Paleo-James River
Area 2
Currituck Slide
Paleo-Roanoke River
Area 3
Intact Slope Strata
Area 4
37°N
36°N
0 20 Kilometers
76°W
75°W

Figure 5

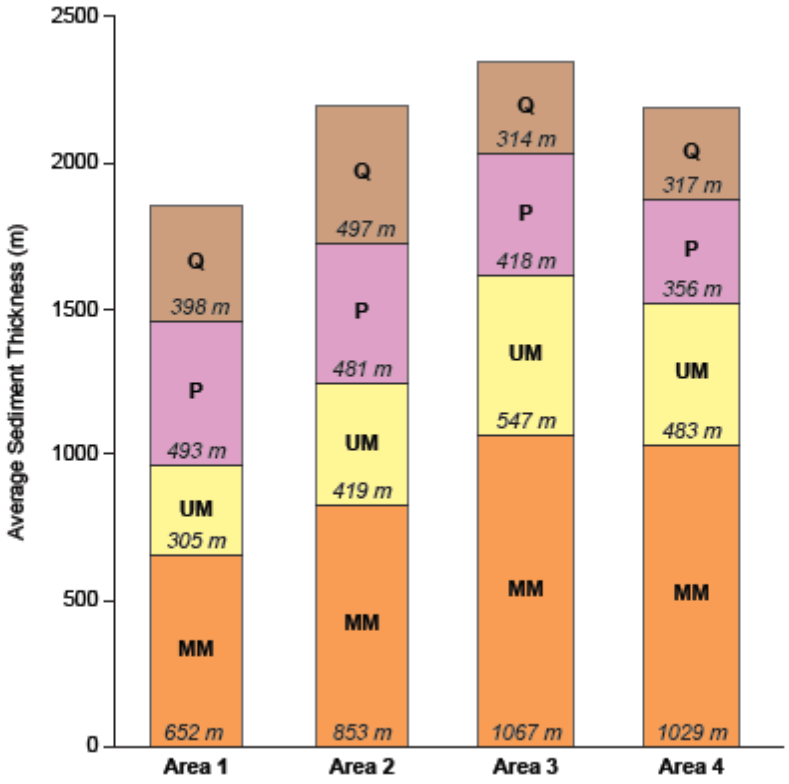
Average Sediment Thickness (m)
2500
2000
1500
1000
500
0
Q
398 m
P
493 m
UM
305 m
MM
652 m
Q
497 m
P
481 m
UM
419 m
MM
853 m
Q
314 m
P
418 m
UM
547 m
MM
1067 m
Q
317 m
P
356 m
UM
483 m
MM
1029 m
Area 1
Area 2
Area 3
Area 4

Figure 6

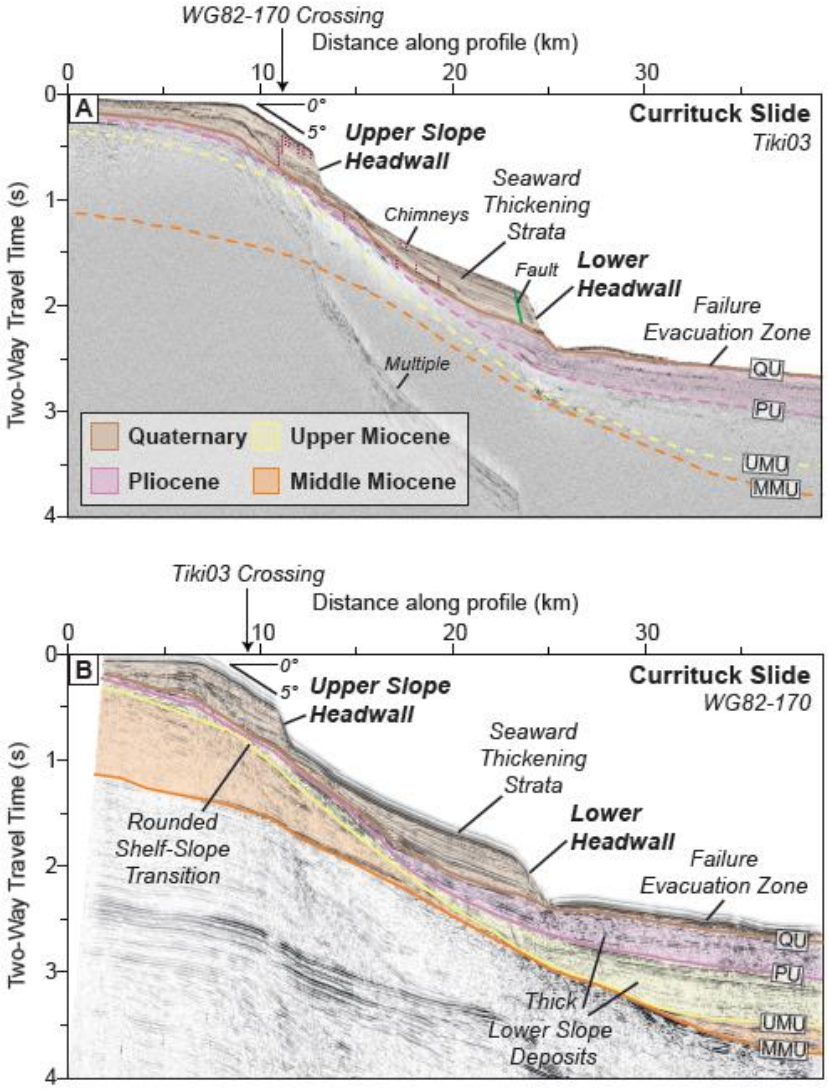
WG82-170 Crossing
Distance along profile (km)
0
10
20
30
A
Currituck Slide
Tiki03
0°
5°
Upper Slope
Headwall
Seaward
Thickening
Strata
Chimneys
Fault
Lower
Headwall
Failure
Evacuation Zone
Multiple
QU
PU
UMU
MMU
Two-Way Travel Time (s)
0
1
2
3
4
Quaternary
Upper Miocene
Pliocene
Middle Miocene
Tiki03 Crossing
Distance along profile (km)
0
10
20
30
B
Currituck Slide
WG82-170
0°
5°
Upper Slope
Headwall
Seaward
Thickening
Strata
Lower
Headwall
Failure
Evacuation Zone
Rounded
Shelf-Slope
Transition
Thick
Lower Slope
Deposits
QU
PU
UMU
MMU
Two-Way Travel Time (s)
0
1
2
3
4

Figure 7

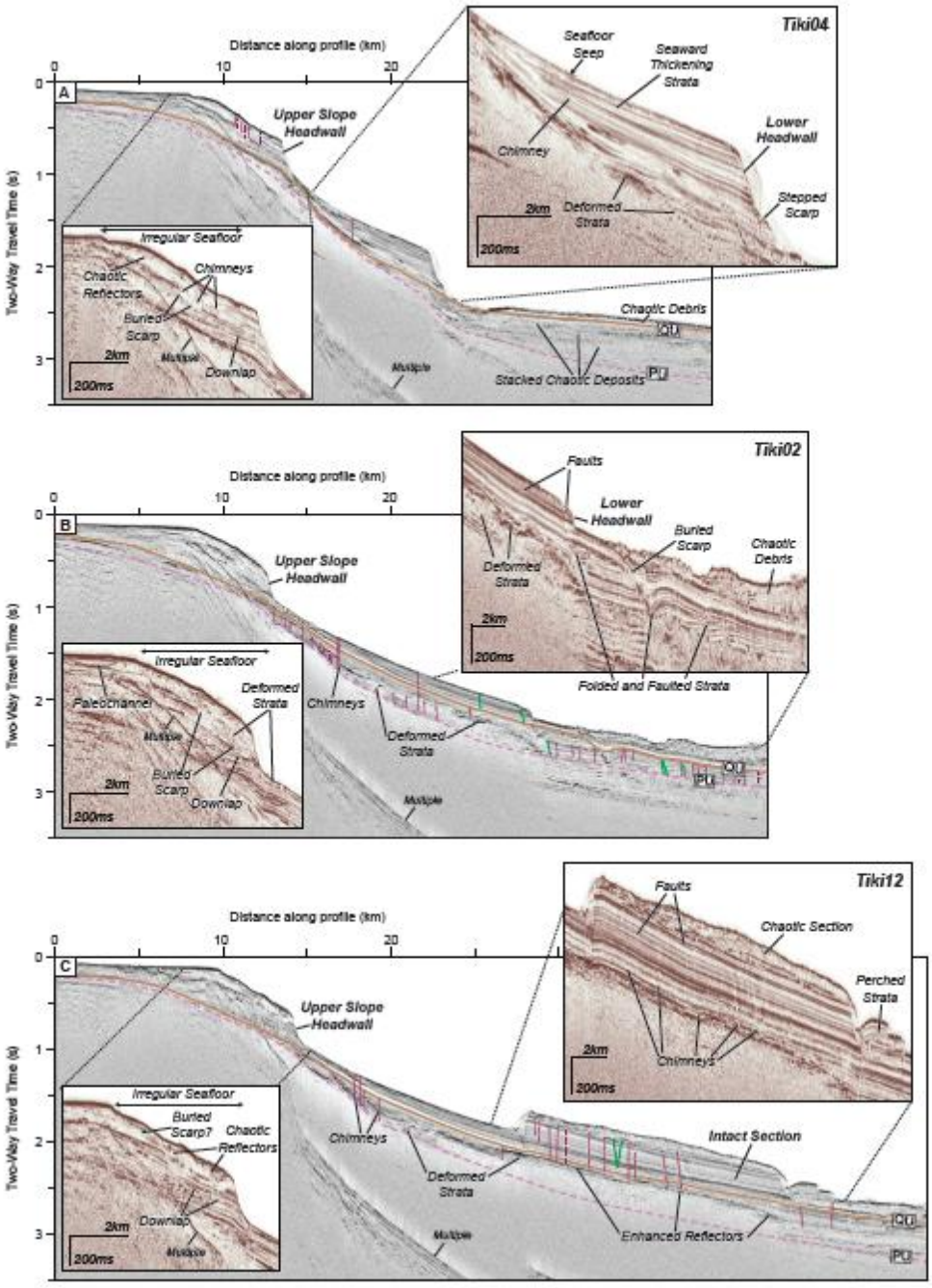
Distance along profile (km)
0
10
20
A
Upper Slope Headwall
Two-Way Travel Time (s)
Tiki04
Seafloor Seep
Seaward Thickening Strata
Lower Headwall
Chimney
Stepped Scarp
2km
Deformed Strata
200ms
Irregular Seafloor
Chaotic Reflectors
Chimneys
Buried Scarp
Multiple
Downlap
Chaotic Debris
QU
Stacked Chaotic Deposits
PU
B
Tiki02
Faults
Lower Headwall
Buried Scarp
Chaotic Debris
Folded and Faulted Strata
Paleochannel
C
Tiki12
Chaotic Section
Perched Strata
Buried Scarp?
Intact Section
Enhanced Reflectors

Figure 8

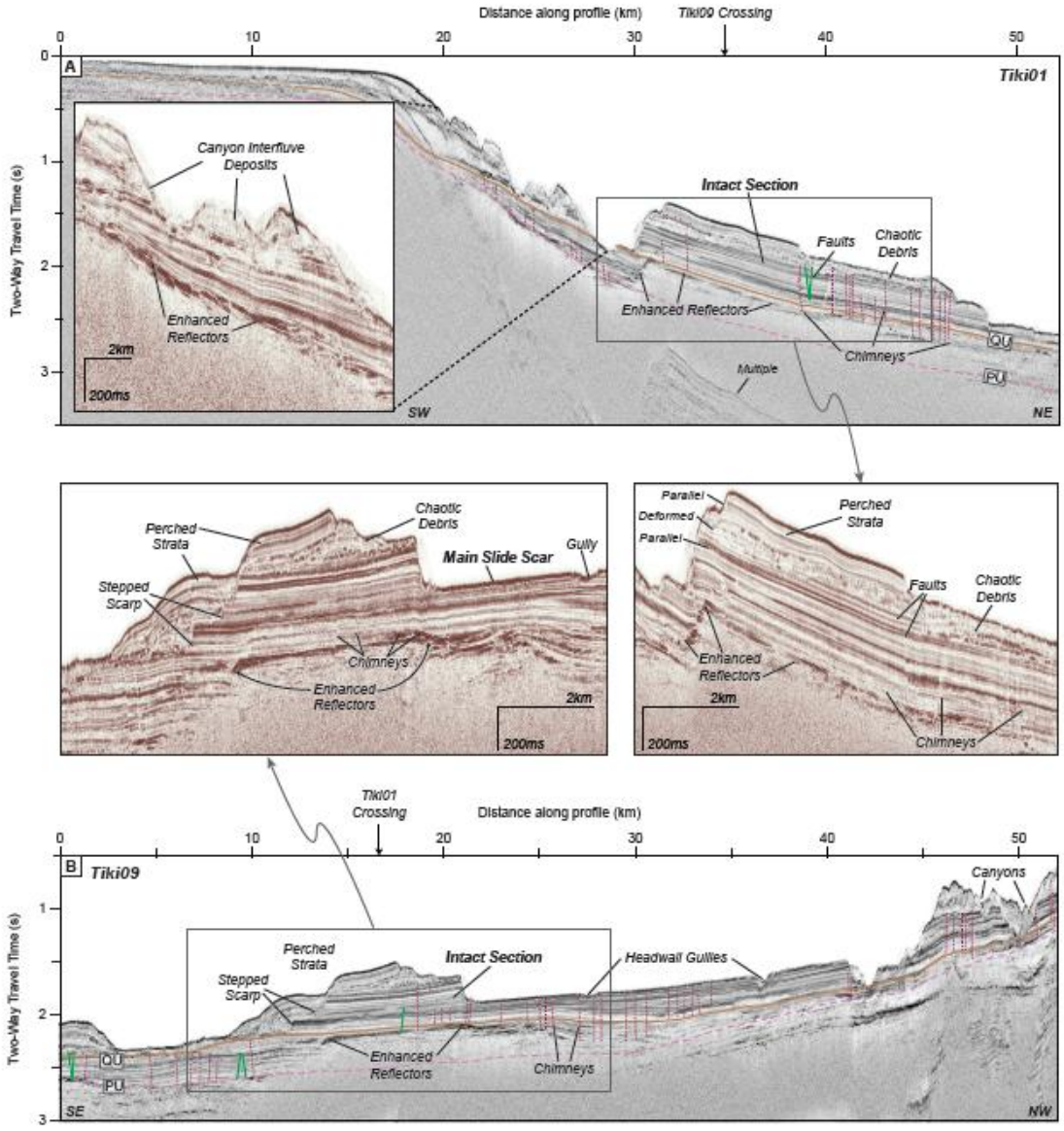
Distance along profile (km)
Tiki00 Crossing
A
Tiki01
Canyon Interfluve Deposits
Enhanced Reflectors
2km
200ms
Intact Section
Faults
Chaotic Debris
Enhanced Reflectors
Chimneys
QU
PU
Multiple
SW
NE
Two-Way Travel Time (s)
Perched Strata
Chaotic Debris
Main Slide Scar
Gully
Stepped Scarp
Chimneys
Enhanced Reflectors
Parallel
Deformed
Parallel
Perched Strata
Faults
Chaotic Debris
Enhanced Reflectors
Chimneys
Tiki01 Crossing
Distance along profile (km)
B
Tiki09
Canyons
Perched Strata
Intact Section
Headwall Gullies
Stepped Scarp
Enhanced Reflectors
Chimneys
QU
PU
SE
NW

Figure 9

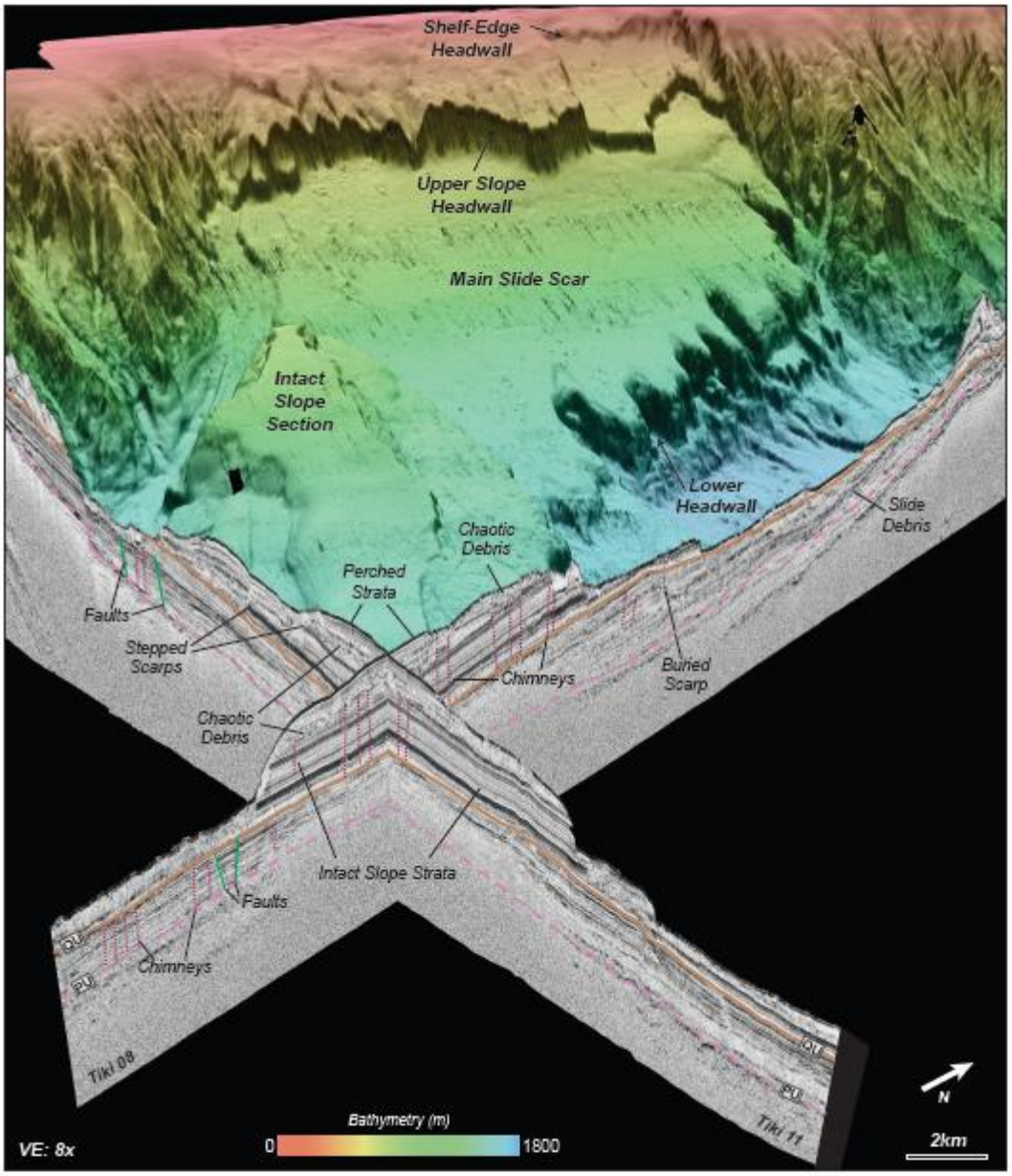
Shelf-Edge Headwall
Upper Slope Headwall
Main Slide Scar
Intact Slope Section
Lower Headwall
Slide Debris
Chaotic Debris
Perched Strata
Faults
Stepped Scarps
Chimneys
Buried Scarp
Chaotic Debris
Intact Slope Strata
Faults
Chimneys
QU
PU
Tiki 08
QU
PU
Tiki 11
Bathymetry (m)
0
1800
VE: 8x
N
2km

Figure 10

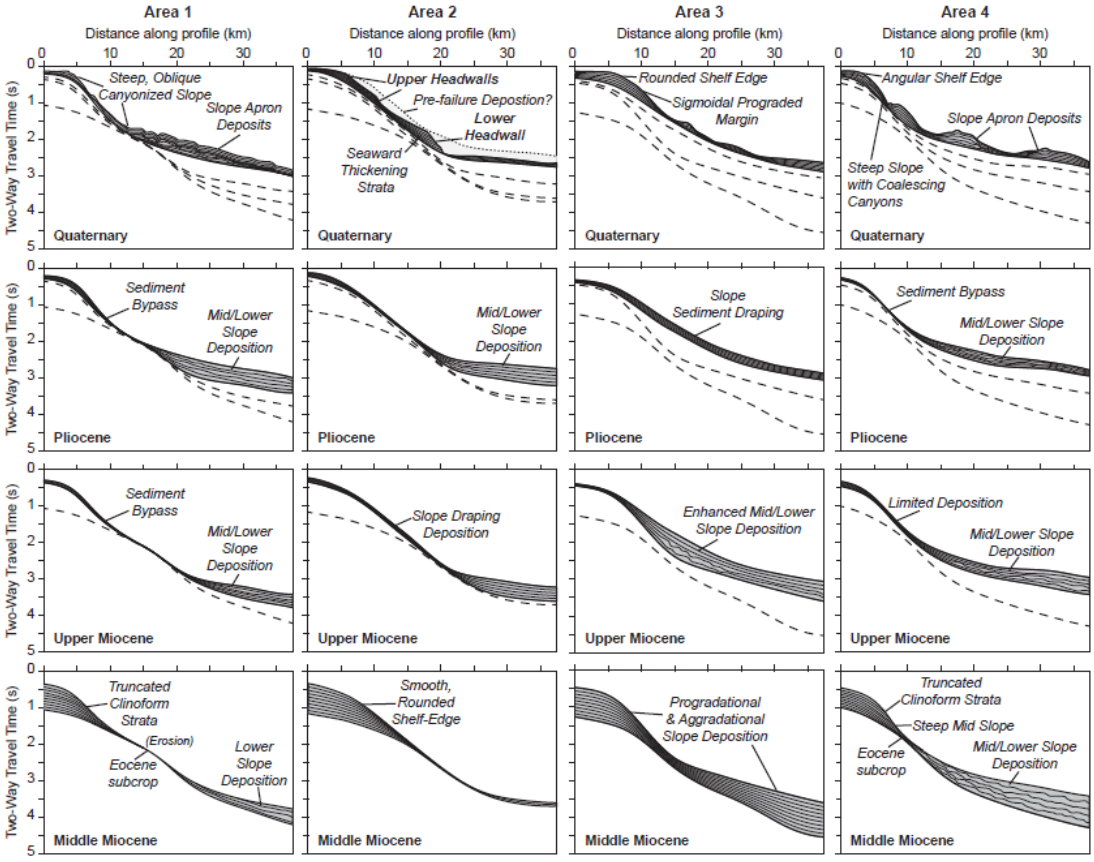
Area 1
Area 2
Area 3
Area 4
Distance along profile (km)
0
10
20
30
Two-Way Travel Time (s)
0
1
2
3
4
5
Steep, Oblique Canyonized Slope
Slope Apron Deposits
Upper Headwalls
Pre-failure Depostion?
Lower Headwall
Seaward Thickening Strata
Rounded Shelf Edge
Sigmoidal Prograded Margin
Angular Shelf Edge
Slope Apron Deposits
Steep Slope with Coalescing Canyons
Quaternary
Sediment Bypass
Mid/Lower Slope Deposition
Slope Sediment Draping
Pliocene
Slope Draping Deposition
Enhanced Mid/Lower Slope Deposition
Limited Deposition
Upper Miocene
Truncated Clinoform Strata
(Erosion)
Eocene subcrop
Lower Slope Deposition
Smooth, Rounded Shelf-Edge
Progradational & Aggradational Slope Deposition
Steep Mid Slope
Middle Miocene

Figure 11